Processing of polymers using reactive solvents

10 Processing of Polymers Using Reactive Solvents

Piet J. Lemstra, Jenci Kurja and Han E. H. Meijer

Centre for Polymers and Composites, Eindhoven Polymer Laboratories,
Eindhoven University of Technology, The Netherlands

List of Symbols and Abbreviations

D_{Ic}	critical interparticle distance
D_n	number-average particle diameter
D_w	weight-average particle diameter
G_c	critical strain energy release rate
G_{Ic}	fracture toughness
ΔH_f	heat of fusion per mole of repeating units
$I(q)$	intensity
M_w	weight-average molar mass
q	scattering vector
Q	experimental invariant
R	gas constant
t_{gel}	gelation time
t_{vitr}	vitrification time
T_B	temperature corresponding to the Berghmans point
T_d	dissolution temperature
T_g	glass transition temperature
T_m	melting temperature of the crystals in the solvent
T_m^0	equilibrium melting point of a pure crystal
T_p	polymerization temperature
T_R	room temperature
V_s	molar volume of solvent
V_u	molar volume of the monomer unit in the polymer chain
η^*	dynamic viscosity
θ	scattering angle (2θ)
λ	wavelength
ρ	electron density
φ, φ_x, φ_A, φ_B, φ_C, φ_D	volume fraction of polymer in polymer–solvent mixture
φ_s	volume fraction of solvent in polymer–solvent mixture
χ	Flory–Huggins interaction parameter
ABS	acrylonitrile–butadiene–styrene graft copolymers
B.P.	Berghmans point
CIPS	chemically induced phase separation
CSAI	compressive strength after impact
CTBN	carboxyl-terminated butadiene–acrylonitrile
DGEBA	diglycidyl ether of bisphenol-A
DGEPPO	diglycidyl ether of polypropylene oxide
DMTA	dynamic mechanical–thermal analysis
EPDM	ethylene–propylene–diene monomer rubber
HDPE	high density polyethylene
HIPS	high-impact polystyrene

IPN	interpenetrating network
LCP	liquid crystalline polymer
L–L	liquid–liquid phase separation
L–S	liquid–solid phase separation
M-CDEA	4,4′-methylene-bis(3-chloro-2,6-diethyl aniline)
MMA	methylmethacrylate
PBT	poly(butylene terephthalate)
PC	polycarbonate
PE	polyethylene
PEI	polyetherimide
PES	poly(ether sulfone)
PETP	poly(ethylene terephthalate)
PMMA	poly(methylmethacrylate)
PP	polypropylene
PPE	poly(2,6-dimethylphenylene ether)
PPO	polypropylene oxide
PPTA	poly-*p*-phenylene-terephthalamide
PS	polystyrene
PSU	polysulfone
SAXS	small angle X-ray scattering
SEM	scanning electron microscopy
TEM	transmission electron microscopy
TIPS	thermally induced phase separation
UCST	upper critical solution temperature
UHMWPE	ultrahigh molecular weight polyethylene
WAXS	wide angle X-ray scattering

10.1 Introduction

Polymer science and technology is the paradigm of a multidisciplinary area. The path from monomer via polymer to functional materials and products travels through the various disciplines of macromolecular science, polymer chemistry and physics, thermodynamics, rheology, processing, and design. The successful design of novel and improved polymeric materials and products requires an integrated approach and a profound understanding of the disciplines met en route. For example, in the past two decades polymer chemists have developed an impressive range of novel polymeric materials, including intrinsically conductive polymers, high glass transition temperature (T_g) polymers with an increased temperature resistance, including liquid crystalline polymers (LCPs), and functional polymers for optical and medical applications. The success of novel present day and future 'speciality polymers', however, in terms of application potential and product design will depend to a large extent on their processability. In this respect many pitfalls have been and will be encountered. For example, intrinsically conductive polymers are rather intractable materials, as well as many newly developed high T_g polymers developed by creative polymer chemists. These intractable polymers often decompose during processing owing to a limited thermal stability at the elevated temperatures required for processing.

As stated above, the successful design of a novel polymeric material and product requires an integrated approach and the close cooperation of specialists from various disciplines, in particular between chemists and process engineers. In the past, several methods have been developed for the processing of intractable polymers. These include blending [e.g., polystyrene with poly(phenylene ether) (PPE)], copolymerization (to reduce the melting or glass transition temperature), and the use of solvents.

All of these methods, however, have specific disadvantages. For example, PPE has a T_g of approximately 215 °C, but it is temperature-sensitive and susceptible to degradation. The PPE/polystyrene system is a classical example of a miscible polymer pair. In practice, PPE is processed by blending with high-impact polystyrene (HIPS). Owing to this miscibility, however, the presence of polystyrene lowers the T_g and consequently the advantage of a high T_g is lost in the final product. In the case of liquid crystalline polymers, notably the aromatic polyesters, copolymerization is commonly used to lower the high melting points of the homopolymers; processable aromatic polyesters are a compromise between ultimate temperature stability and processability (Blackwell and Biswas, 1987). If no chemical compromise is made between the ultimate properties and the processability, solvents can be used to facilitate processing, as in the case of the aromatic polyamides. Poly-*p*-phenylene-terephthalamide (PPTA) is the base material for the well-known Kevlar and Twaron high-performance fibers which are obtained by spinning from nematic solutions (Ciferri, 1987). Other, more classical, examples in this respect are fibers based on polyvinyl alcohol and polyacrylonitrile. The use of solvents, however, is generally limited to products with a high surface-to-volume ratio, such as fibers, coatings, and pre-impregnated (pre-pregs) materials for composite applications, and has one major disadvantage: the solvent usually has to be removed completely after processing, which is increasingly cumbersome in view of environmental legislation.

Within the Centre for Polymer Composites of Eindhoven Polymer Laboratories, a project was started in the early 1990s to

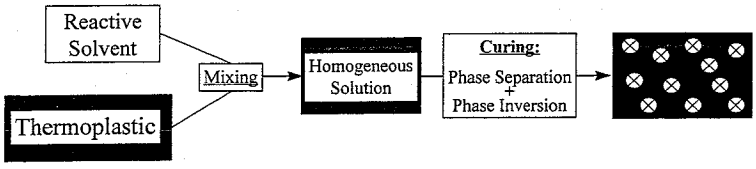

Figure 10-1. Schematic outline of processing with reactive solvents.

explore the possibility of using reactive solvents to facilitate the processing of intractable polymers. Figure 10-1 shows schematically the basic principles of processsing with reactive solvents. A thermoplastic polymer is dissolved, usually at elevated temperatures, in a reactive solvent (monomer). The homogeneous solution is transferred into a mold or into a fabric, as in the case of composites. Upon curing in the mold, phase separation and phase inversion occur since the two polymers are immiscible, and the polymer concentration in the initially homogeneous solution is chosen such that the originally dissolved polymer becomes the continuous matrix phase. After curing, the polymerized reactive solvent (monomer) is dispersed as a particulate phase in the matrix. For example, PPE dissolves in epoxy (resin) at elevated temperatures. The PPE/epoxy (resin) solution, containing a hardener, can be transferred into a mold where, upon curing, phase separation and phase inversion occur and the cured epoxy is dispersed as thermoset particles in the continuous PPE matrix.

The obvious advantages of using reactive solvents are discussed in detail in subsequent sections. The viscosity and processing temperatures when using a reactive solvent are low in comparison with the case of pure PPE (see Fig. 10-2 and later), and consequently thermal degradation can be prevented. After curing, the continuous matrix is PPE and hence the properties of the composite system are dominated by this polymer. The reactive solvent remains in the system and there is no need for solvent

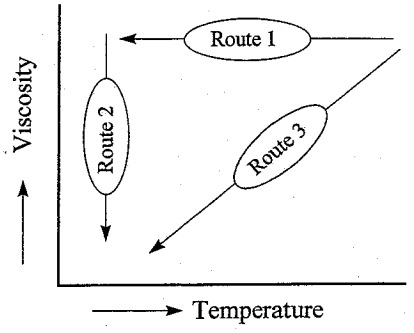

Figure 10-2. Schematic temperature–viscosity diagram.

removal! Moreover, the cured reactive solvent can even be a useful constituent, for example, if rubbery epoxies are used, the dispersed phase can be used to toughen the material (Venderbosch, 1995; Venderbosch et al., 1995 a, b), see also Sec. 10.5.

During the course of our investigations, we have found many polymer–reactive solvent systems which have proved to be suitable for this novel processing technique. In fact, processing with reactive solvents showed not only to be of interest for intractable polymers, but also for standard tractable polymers like polyolefins and rubbers. Dissolving polyethylene, for example, in a reactive solvent like styrene renders it possible to obtain low viscosity 'pourable' polyethylenes and to make very large and complex-shaped parts, which cannot normally be obtained via injection molding.

As will be discussed in subsequent sections, epoxy resin is often used as a reactive solvent in our processing route. Epoxy resins are well-known solvents for many polymers and thermoset epoxies are often tough-

ened by dissolving rubbers or even high T_g thermoplasts. Liquid rubbers, for example, carboxyl-terminated butadiene–acrylonitrile (CTBN) rubbers, can be dissolved in epoxy resins and upon curing phase separation occurs (Garg and Mai, 1988; Levita, 1989). Instead of rubbers, thermoplastic additives have been used to toughen cured epoxy resins like poly(ether sulfone) (PES) and poly(ether imide). The advantage of high T_g polymers over rubbers is that toughening is not achieved at the expense of the stiffness of the cured epoxy resin. However, compared with conventional rubber toughening, the glassy thermoplastic dispersed particles are less capable of initiating yielding in the surrounding matrix. Consequently, the use of high T_g thermoplastics as additives in epoxy resins is limited to densely crosslinked systems, since these systems are not capable of yielding; consequently, an increased toughness depends on secondary toughening mechanisms, such as particle tearing, crack bridging, and crack bifurcation (Mülhaupt, 1990; Pearson, 1993; Hedrick et al., 1993). The difference between the method for toughening epoxies and the novel processing route described in this chapter, involving epoxy resin as a solvent, is that in the former case phase separation is induced chemically, but no phase inversion is attempted; the thermoset epoxy is and remains the continuous matrix phase.

Last, but not least, a method that comes close to the processing route with reactive solvents is the synthesis of interpenetrating networks (IPNs), notably the semi-IPNs, where one polymeric constituent is crosslinked and the other constituent remains linear (Sperling, 1994). However, an IPN should possess, to some extent, a certain degree of molecular interpenetration. In our process of using reactive solvents, no explicit attempts are made to pursue interpenetration of the various phases. In fact, in the system PPE/epoxy (resin), the chemically induced phase separation is virtually complete (Venderbosch, 1995). The use of reactive solvents provides the potential to extend the processing characteristics of thermoplastic polymers beyond their existing limits. This concept can be employed for both intractable and tractable polymers. In principle, there are two major advantages, as shown in Fig. 10-2.

The use of reactive solvents can reduce the processing temperature (route 1), thus preventing thermal degradation in the case of intractable polymers, or reduce the viscosity (route 2) in the case of tractable polymers. In actual practice, route 3 is usually followed, providing a reduction in both the processing temperature and the viscosity. The application of reactive solvents thus enables alternative processing routes, such as processing intractable polymers and pouring or casting standard polymers, operations where a low viscosity is a prerequisite. In this chapter, the processing route with reactive solvents will be discussed for various systems, including PPE/epoxy resin (Sec. 10.5), poly(methylmethacrylate)/epoxy (Sec. 10.6.1), and polyethylene/styrene (Sec. 10.6.2).

10.2 Classification of Synthetic Polymers

Synthetic polymers/plastics are typical materials of the 20th century, and they have displayed an enormous growth in production in the past few decades. Currently, approximately 100 million tonnes are produced annually. Considering their low specific mass (ca. $900-1500\ kg/m^3$), plastics are approaching steel in terms of production volume. Based on their molecular structure, synthetic polymers can be subdivided into

three main categories: thermoplastics, thermosets, and synthetic rubbers.

10.2.1 Thermoplastics

In terms of production volume, the majority of present-day polymers belong to the class of thermoplastics. The adjective thermoplastic is indicative of the processing of these polymers. Thermoplastic polymers are obtained from the chemical industry, where specific monomers are polymerized under controlled conditions and supplied to the converter in the form of pellets and sometimes powder. These are transformed into products by the converter by heating/melting, shaping (extrusion/molding), and cooling (crystallization/vitrification). An impressive range of thermoplastic polymers is available nowadays, and molecular structures can be fine-tuned by proper control of the catalyst and the polymerization in the reactor in order to obtain an optimum structure and performance. It is beyond the scope of this chapter to discuss in detail current trends and product ranges, and consequently we limit ourselves to a discussion on polymers that are relevant to the novel reactive processing technique. Thermoplastic polymers can be subdivided into three categories: bulk or commodity plastics, engineering plastics, and speciality polymers. In Fig. 10-3, these three classes are represented in a product triangle.

The commodity plastics are the most important class of present-day thermoplastic polymers and constitute over 70% of the total synthetic polymer production [approximately 50 million tonnes of polyolefins (PE and PP), and about 25 million tonnes of polyvinyl chloride and polystyrene]. Polyethylene (PE) and polypropylene (PP) are, in fact, only generic names, representing an entire family of polymers which usually differ in molecular characteristics, e.g., molar mass distribution, homopolymers or copolymers, stereoregularity (PP), etc. The commodity plastics may at first sight appear to be rather low-tech and well-established comprising a full range of types and subtypes, tailored for the end-user and well-defined application areas. However, the field of commodity plastics is, after the discovery of the stereospecific polymerization of olefins by Ziegler and Natta in the mid-1950s, once again in a revolutionary stage due to the introduction of metallocene catalysis. After a developmental period of

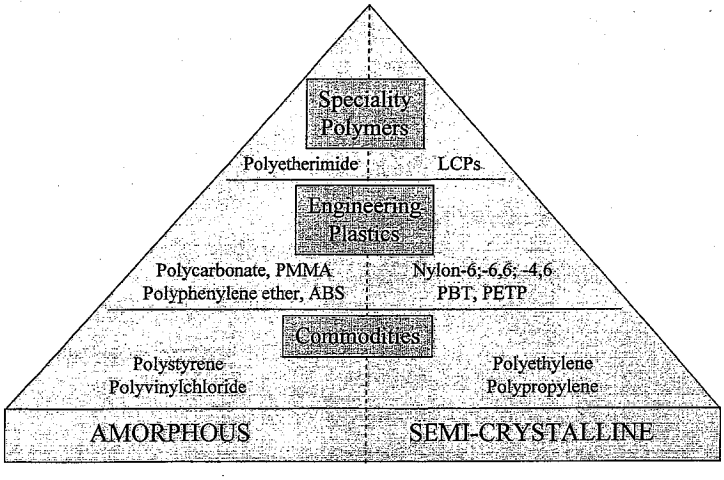

Figure 10-3. The three classes of thermoplastic polymers (See the List of Symbols and Abbreviations for an explanation of the different acronyms.)

approximately 25 years (1970–1995), metallocene 'single-site' catalysts have been introduced into the chemical reactor, providing the opportunity to produce novel types of polyolefins (Thayer, 1995). For example, very low density polyethylene ('plastomers') can be produced. Syndiotactic polypropylene and syndiotactic polystyrene can be made on a technologically feasible scale, whereas novel copolymers based on ethylene and cyclic olefins possessing T_gs well above 100 °C have recently been introduced.

At first glance, there seems to be no need to use (reactive) solvents for processing commodity plastics in view of the well-established processing techniques and the large range of (sub)types on the market, which are tailored for specific applications. However, there are a few exceptions, including UHMWPE (ultrahigh molecular weight polyethylene), which is a linear polyethylene grade possessing, according to ASTM definitions (D4020), a molar mass of at least 3000 kg/mol. UHMWPE products are usually obtained by machining semi-finished stock, which is obtained by compression molding (sintering) or ram extrusion. Solvents are used, however, for UHMWPE fibers produced by DSM (DYNEEMA) and its licensee, Allied Signal (SPECTRA). These high-performance polyethylene fibers are obtained by solution(gel)-spinning and are described in detail by Bastiaansen in Chap. 11 of this Volume.

To the best of our knowledge, the use of *reactive* solvents in processing commodity plastics has not been exploited. Nevertheless, some preliminary results will be presented in Sec. 10.6.2 concerning the processing of polyethylene using reactive solvents.

Engineering plastics are typically polymeric materials with an improved temperature resistance (related to a higher T_g) and mechanical response compared with commodity plastics. In the field of engineering plastics, a distinction is usually made between amorphous and semicrystalline plastics. Typical examples of semicrystalline engineering plastics are the polyamides (most notably nylon-6, -6,6, and -4,6) and polyesters such as PETP and PBT. Well-known amorphous engineering plastics are ABS, PC, PMMA, and PPE (for an explanation of the abbreviations, see the List of Symbols and Abbreviations). In Sec. 10.5, the use of reactive solvents with respect to the processing of intractable polymers, most notably PPE, will be discussed, aimed at enhanced processability, while in Sec. 10.6, the processing of tractable polymers, e.g., PMMA and HDPE will be discussed. In the case of PMMA, the major aim is to introduce specific product properties.

Speciality polymers are polymers with very specific properties. Typical examples of speciality polymers are high T_g polymers such as PEI and PSU, and polymers which become intrinsically conductive after doping (e.g., polyaniline and polypyrrole). Owing to their high T_g, polymers like PEI and PSU seem to be suitable candidates for processing with reactive solvents. Up to now, no significant literature data are available concerning the processing of high T_g polymers with reactive solvents.

10.2.2 Thermosets

Thermosets are obtained by polymerizing (curing) low molar mass resins (monomers with a functionality >2). For this reason, the viscosity of thermoset resins before curing is initially low. For example, the viscosity of a standard bisphenol-A epoxy resin at 25 °C is of the order of 10 Pa s. This low initial viscosity is useful in applications such as coatings, adhesives, and for impregnation of pre-pregs in the preparation of

fiber-reinforced composites. Curing is often achieved by the addition of curing agents and/or initiators, and eventually a chemical network is formed. Depending on the functionality of the starting resin, a more or less densely crosslinked system is obtained. Typically, the curing procedure is performed by the end-user during in-mold shaping. In view of the fact that thermosets are crosslinked systems after curing and low viscosity resins before curing, processing with reactive solvents is not of direct interest. However, some resins, e.g., the epoxies, can be very useful reactive solvents themselves, as shown in (Secs. 10.5 and 10.6).

10.2.3 Rubbers

Rubbers are materials that possess elastomeric properties, i.e., they can be stretched reversibly to high extension ratios. Elastomeric properties are related to the flexibility of the polymer chains, which are lightly crosslinked to prevent permanent flow. The processing of green (uncrosslinked) rubbers using reactive solvents is possible in principle [e.g., EPDM rubber with styrene (pourable rubbers)]. To the best of our knowledge, no data are available concerning the processing of rubbers with reactive solvents, at least not within the concept of the present technique. Rubbers, however, are dissolved in reactive solvents (monomers) in the reactor, and during polymerization, phase separation and inversion take place, resulting in rubber-modified pellets or powders. Two typical examples of rubber-modified polymers are high-impact polystyrene (HIPS) and ABS. HIPS is prepared by dissolving polybutadiene in styrene, after which the styrene is polymerized under continuous agitation. This results in a morphology in which polystyrene forms the continuous phase and polybutadiene the dispersed phase, containing small domains of polystyrene. A similar procedure is applied in the preparation of ABS copolymers.

It is important to note that for these rubber-modified polymers, which are formed in the reactor, the morphology is stabilized by grafting and crosslinking of the dispersed rubbery phase. Consequently, upon subsequent processing, the induced morphology does not change significantly. With respect to the processing of polymers with reactive solvents, however, the morphology is obtained in the mold, which has important consequences for handling and subsequent processing (see Sec. 10.7).

10.3 Guidelines for the Selection of a Reactive Solvent

Like polymers, reactive solvents can be classified according to their potential use in polymeric materials derived from them. However, it is more common to classify monomers according to the polymerization mechanism that converts them into a polymer, i.e., a chain-growth or a step-growth polymerization mechanism (Bikales, 1985). Among the important thermoplastics produced by a *chain-growth* type of polymerization, are polymers such as polyethylene, polypropylene, and polystyrene. Via the nature of the propagating species, variations in the polymer microstructure can be achieved, such as block copolymers and stereoregular polymers. During chain-growth polymerization, the monomer present adds to a propagating polymer chain, thus extending the chain by one monomeric unit per propagating step.

In the case of *step-growth* polymerization, however, the polymer chain is formed not exclusively via the addition of monomer to a growing polymer chain, but also via the

combination of monomer, oligomer, or polymer molecules with other monomer, oligomer, or polymer molecules. Step-growth polymerizations can be performed in the so-called condensation or addition mode. During polycondensations, molecules are linked via a condensation reaction, upon which a small molecule is released, e.g., water. In the case of polyadditions, on the other hand, the separate monomers are linked via addition reactions, resulting in a polymer chain that is a perfect sum of all the atoms in the monomers. Typical examples of polycondensations are the formation of polyesters and polyamides, while the reaction between amines and epoxies, or diisocyanates and diols can be designated as a polyaddition.

The major differences between step-growth and chain-growth polymerizations are:

1. During step-growth polymerizations, reactive groups are consumed during the polymerization, whereas in chain-growth polymerizations the reactive groups are continuously generated during the polymerization process. At any instance, the chain-growth polymerization system contains unreacted monomer, while this is not necessarily true for a step-growth polymerization.
2. The average molar mass of the polymer formed during step-growth polymerization is a function of the conversion, and a high molar mass polymer is only formed at very high conversions. The polymer formed during a chain-growth polymerization, on the other hand, already has a high molar mass at low monomer conversions. These differences between chain-growth and step-growth polymerizations, especially the difference in the development of the molar mass of the polymer formed during polymerization of the reactive solvent, have a profound effect on the phase behavior of the polymer-reactive, solvent-polymerized, reactive solvent system (see also Secs. 10.5 and 10.6).

Based on this, the following can be said with respect to the mode of polymerization by which the reactive solvent can be transformed to polymer, and concomitantly the choice of reactive solvent for a specific system: Concerning step-growth polymerizations, polycondensations are less favorable than polyadditions, since the molecules that are eliminated during a polycondensation can cause problems in the end products, e.g., the small molecule released during polymerization can act as a plasticizer for the continuous and/or dispersed phase. Further, chain-growth type polymerizations offer greater possibilities for controlling the molecular microstructure of the polymer formed, e.g., semicrystalline, amorphous, or rubbery, by changing the monomer(s), and/or the mode of initiation/propagation, than step-growth polymerizations.

For instance, epoxy resins fulfill the above criteria very well, as has been demonstrated by Venderbosch (1995) and Venderbosch et al. (1994, 1995 a, b) (see also Sec. 10.5). Some commercially available epoxy resins are shown in Fig. 10-4; DGEBA has an aromatic and DGEPPO an aliphatic backbone. These epoxy resins can be cured using different curing agents, for example, poly(propylene oxide) diamine (Jeffamine D-400) or the sterically hindered, and thus slow, 4,4′-methylene-bis(3-chloro-2,6-diethyl aniline) (M-CDEA) (see Fig. 10-4). The curing utilizing aromatic epoxy resins (A) results, at high crosslink densities, in high T_g, brittle, thermoset epoxies, whereas the aliphatic epoxy resins (B) exhibit elastomeric properties after curing (see also Secs. 10.5 and 10.6).

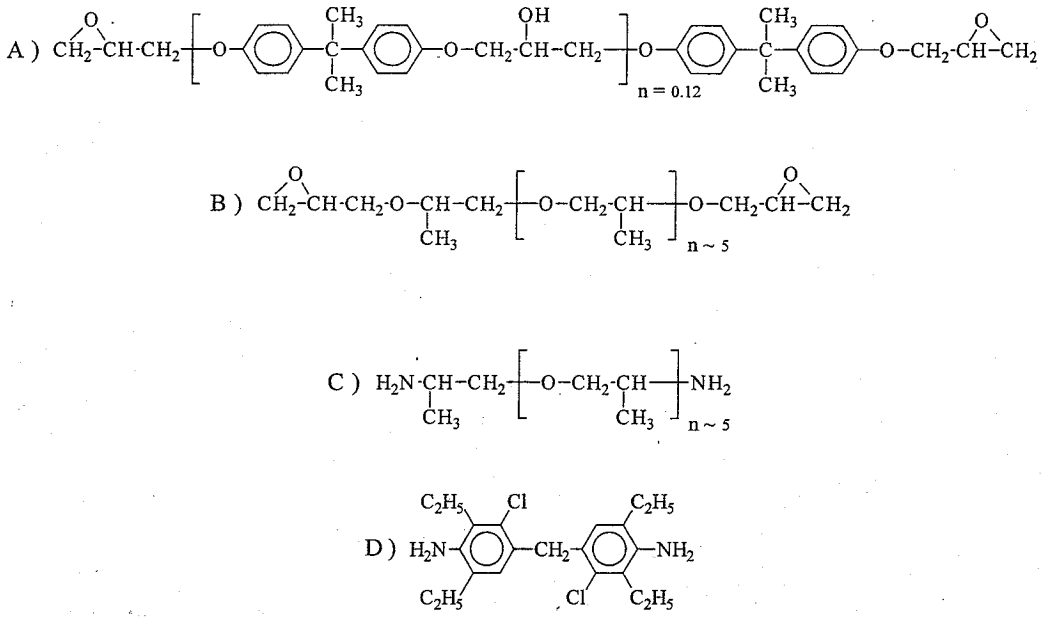

Figure 10-4. Structural formulae of: (A) DGEBA, (B) DGEPPO, (C) Jeffamine D-400, and (D) M-CDEA.

10.4 Basic Aspects of Processing with Reactive Solvents

During the processing of polymers with reactive solvents, it is of importance to know the phase behavior of the particular polymer/reactive solvent system. Processing of the polymer and reactive solvent should proceed in the homogeneous state, i.e. the polymer should be dissolved. In the mold, upon curing, complex changes take place due to chemically induced phase separation and inversion. To some extent, these complex morphological changes due to chemically induced phase separation (CIPS) are similar to the morphology development during thermally induced phase separation (TIPS). Therefore, in this section, TIPS will be discussed first, for amorphous as well as semicrystalline polymers, to provide the basics for understanding the more complex phenomena that occur during CIPS.

10.4.1 Phase Behavior of Amorphous Polymers in Solution

In the case of an amorphous polymer, the T_g will be lowered in the presence of a (good) solvent. The solvent acts as a plasticizer and the T_g decreases with increasing solvent content. Couchman (1983) has developed a thermodynamic approach for predicting the glass transition temperature of polymer mixtures, but in actual practice the simpler Fox equation (Fox, 1956), [see Eq. (10-1)] is often used to describe the T_g reduction in the presence of a solvent. In Eq. (10-1), φ represents the volume fraction of the polymer in the polymer–solvent mixture.

$$\frac{1}{T_g(\varphi)} = \frac{(1-\varphi)}{T_g^{\text{Solvent}}} + \frac{\varphi}{T_g^{\text{Polymer}}} \qquad (10\text{-}1)$$

Depending on the solvent quality, various situations can be encountered, as shown schematically in Fig. 10-5 A and B.

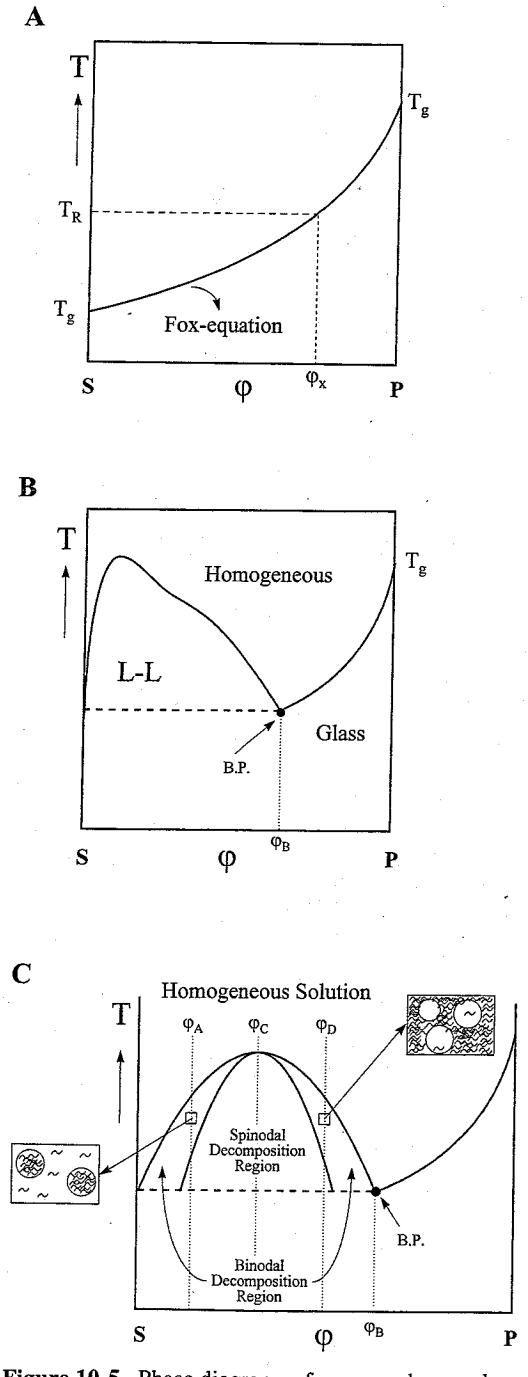

Figure 10-5. Phase diagrams of an amorphous polymer (P) and a solvent (S) for (A) a system with a polymer and a good solvent and (B) a system with a polymer and a poor(er) solvent. (C) Illustration of the morphology development during different phase separation mechanisms.

In the case of a good solvent (Fig. 10-5 A), the T_g decreases with increasing solvent concentration and below φ_x a homogeneous solution is obtained at room temperature, T_R. Above φ_x, the solution will vitrify into a homogeneous glass upon cooling to room temperature. In the case of a poor solvent, the phase diagram can become more complex. The T_g curve often interferes with a liquid–liquid demixing curve, as shown in Fig. 10-5 B. The intersection point, where the T_g composition curve intersects with the L–L demixing or cloud-point curve, is called the Berghmans point, B. P. in Fig. 10-5 B, named after Prof. H. Berghmans (KU-Leuven), who noticed the importance of this intersection point for the phase behavior of polymer solutions (Arnauts et al., 1993). At a concentration φ higher than φ_B, the homogenous solution vitrifies upon cooling below the T_g curve, as discussed previously for Fig. 10-5 A. At concentrations lower than φ_B, the homogeneous solution will become metastable upon cooling into the L–L demixing region. From a purely thermodynamic point of view, the most favorable and final equilibrium situation will be the separation into two coexistent macroscopic phases, respectively a dilute and a concentrated polymer/solvent phase. This process, however, is rather slow in polymer systems. If the temperature, upon cooling, passes, T_B (the temperature corresponding to the Berghmans point) the metastable solution will vitrify if continuity of the glassy phases (domains) is present in the system, usually at higher polymer concentrations, or vitrified particles will separate from solution at lower concentrations. The formation of a vitrified gel or the precipitation of vitrified particles is, as mentioned earlier, dependent on the polymer concentration in solution.

Although a detailed thermodynamic description is beyond the scope of the

present chapter, we will briefly address some details. In the case of thermally induced phase separation, a distinction must be made between binodal and spinodal decomposition. In practice, we are dealing with multicomponent systems, since polymers are usually polydisperse materials with a broad molar mass distribution. In these polydisperse systems, the critical point is not on the top of the cloud-point curve but shifted somewhat to the right, and the cloud-point curve is usually indented, as shown in Fig. 10-5 B (Koningsveld et al., 1996).

In order to illustrate the morphology development and its dependence on the mechanism of phase separation, i.e., binodal or spinodal, Fig. 10-5 C shows that in the case of a binodal system (monodisperse polymer and solvent), the critical point is at the top of the cloud-point curve, where the binodal and spinodal curves meet. Upon cooling from the homogeneous solution, either spinodal (through the critical point) or binodal demixing occurs.

In the case of binodal demixing, phase separation proceeds through nucleation and growth of the minor phase. Cooling a solution with a polymer concentration φ_A, into the binodal region will result in the precipitation of (spherical) particles. The overall polymer concentration is too low to provide material continuity. Upon cooling a solution with a polymer concentration, φ_D, the concentrated polymer phase will form the continuous matrix which will then vitrify at the temperature corresponding to the Berghmans point, T_B. In the case of spinodal decomposition (φ_C), spontaneous phase separation occurs via concentration fluctuations. The word spontaneous does not mean that phase separation via spinodal decomposition is an instantaneous process. According to the Cahn–Hilliard theory (Cahn, 1963), concentration fluctuations develop and the fluctuation length with the highest growing rate (the most dominant wavelength) results in the most-frequently found domain size. At the start of the demixing process, interconnectivity (co-continuous structure) prevails, but gradually the texture coarsens, approaching an ultimate separation into two macroscopic phases (Fujita, 1990). However, this situation is not reached, since the system vitrifies upon cooling below the temperature corresponding to the Berghmans point.

10.4.2 Phase Behavior of Semicrystalline Polymers

In the case of semicrystalline polymers, we have to focus on the melting temperature T_m instead of T_g. The melting point depression due to the presence of solvent(s) is usually described by the well-known melting point depression relationship, which reads for high molar mass polymers (Flory, 1956)

$$\frac{1}{T_m} - \frac{1}{T_m^0} = \frac{R}{\Delta H_f} \times \frac{V_u}{V_s}(\varphi_s - \chi\varphi_s^2) \qquad (10\text{-}2)$$

In Eq. (10-2), T_m represents the melting temperature, or equivalently the dissolution temperature, of the crystals in the solvent, T_m^0 is the equilibrium melting point of the pure crystal, R is the gas constant, φ_s the volume fraction of solvent, χ the Flory–Huggins interaction parameter, V_u the molar volume of the monomer unit in the polymer chain, V_s the molar volume of the solvent, and ΔH_f is the heat of fusion per mole of repeating units.

Figure 10-6 A shows the melting point depression of a polymer crystal in equilibrium with the surrounding solution. Equation (10-2) is only applicable to concentrated and semidilute systems, and consequently the far left part of the phase diagram is represented by a dotted line. The melting point of the polymer is lowered by the pres-

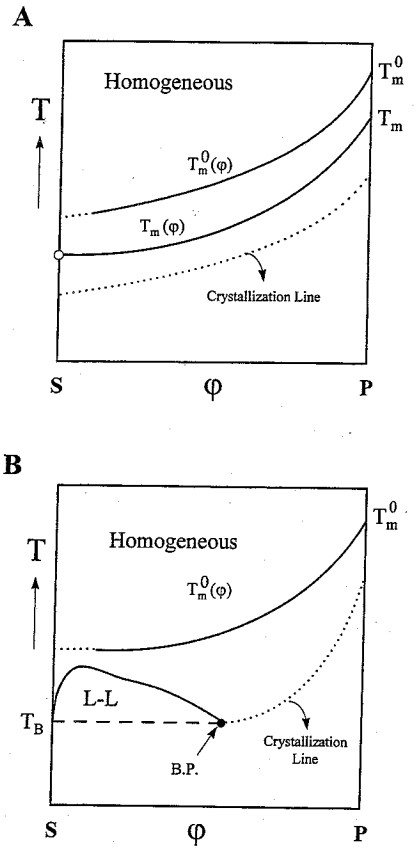

Figure 10-6. Phase diagrams of a semicrystalline polymer and a low molar mass solvent for (A) a system in which the solvent is a good solvent for the polymer and (B) a system in which the solvent is a poor(er) solvent for the polymer.

ence of a solvent, and vice versa, i.e., the melting point of the solvent is lowered by the presence of the polymer. Consequently, a eutectic point is to be expected. However, as shown by Smith (1976), a eutectic point is not observed if the difference between the melting point of the polymer and the solvent exceeds 100 K. In Fig. 10-6 A, the melting point of the solvent is not indicated in view of the fact that in the systems to be discussed below, the melting point of the solvent is far below room temperature and the difference between the melting point of the polymer and the solvent is >100 K.

It is important to note that the equilibrium curve $T_m(\varphi)$ in Fig. 10-6 A is never obtained experimentally. Equilibrium refers to perfect, large crystals, i.e., so-called extended-chain crystals in the case of polymers. In practice, however, polymer crystals consist of folded-chain crystals and the fold length, or equivalently the thickness of the folded-chain crystals is of the order of 10–30 nm. These imperfect and small crystals melt or dissolve at a lower temperature, as indicated in Fig. 10-6 A by the curve $T_m(\varphi)$; in the literature the melting point is given as T_m to distinguish it from the equilibrium melting point, T_m^0.

The experimental $T_m(\varphi)$ curve as drawn schematically in Fig. 10-6 A should approach the melting point of the pure solvent when the polymer concentration approaches zero. In Fig. 10-6 A, the intersection of the experimental melting (dissolution) $T_m(\varphi)$ curve with the temperature axis is represented by an open circle. Melting (dissolution) of polymer crystals at low concentrations is currently, yet again a matter of debate (Nies and Berghmans, 1996). When the polymer concentration approaches zero, the melting point T_m should approach the melting point of the solvent. However, it is found in practice that the melting point T_m becomes independent of the polymer concentration when φ approaches zero. The reason for this is probably that upon melting (dissolution) of a polymer crystal, the polymer chain goes from a folded-chain conformation within the crystal to a random-coil chain in solution. The random coil in solution has its own local concentration, i.e., upon dissolution the chain experiences a low but finite local concentration of the order of a few percent, related to the coil dimensions. Consequently, the melting (dissolution) temperature remains constant at low φ, i.e., the local concentration of a random coil.

Crystallization is a nucleation-controlled process and only occurs at a certain degree of supercooling, as indicated by the crystallization line in Fig. 10-6 A. For crystallizable polymers in solution, crystallization can also interfere with liquid–liquid demixing. This is depicted schematically in Fig. 10-6 B. The L–L demixing curve can be located above or below the equilibrium melting curve, $T_m^0(\varphi)$. The latter case is shown in Fig. 10-6 B. Even if the L–L demixing curve is below the equilibrium dissolution curve, $T_m^0(\varphi)$, L–L demixing usually occurs before crystallization, since the crystallization process is a slower process and requires a certain degree of undercooling. Instead of vitrification, the concentrated domains will crystallize upon cooling below the temperature T_B.

10.4.3 Thermally Versus Chemically Induced Phase Separation

As noted before, the morphology development during thermally induced phase separation (TIPS) is very similar to the morphology development during chemically induced phase separation (CIPS) (see Fig. 10-7 A and B, respectively). The reason is that upon curing a polymer/reactive solvent system, the polymerized reactive solvent becomes immiscible with the dissolved polymer and phase separation should occur at some stage during the curing (polymerization) step.

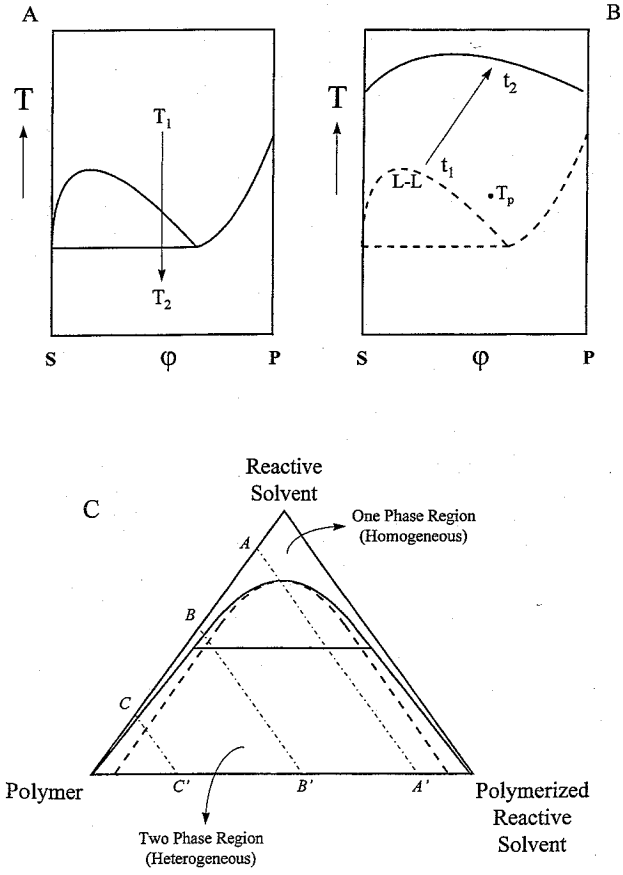

Figure 10-7. Schematic representation of the changes in miscibility of a polymer in a poor solvent in the case of (A) cooling from T_1 to T_2 (TIPS), (B) isothermal polymerization of the reactive solvent from t_1 to t_2 (CIPS), and (C) a ternary phase diagram of the polymer–polymerizing reactive solvent system. Lines A–A′, B–B′, and C–C′ represent polymerization lines, and the horizontal line is a tie line connecting the coexisting phases.

There is, however, one important difference between TIPS and CIPS. In the case of TIPS, a two-phase system will be formed, consisting of a dilute and a concentrated polymer phase, either in the form of two separate macrophases or in microdomains if vitrification occurs, i.e., cooling below the Berghmans point. In the case of CIPS, liquid–liquid demixing will occur due to immiscibility of the originally dissolved polymer and the polymer that is formed during polymerization (curing). Coarsening of the structure is strongly surpressed by an increase in the viscosity, induced by phase separation and the polymerization reaction. Moreover, fixation of the structure via vitrification, crystallization, or crosslinking will prevent the formation of two macrophases. Another important difference from TIPS is that phase separation is complete, or at least should be attemped, not in the sense of the formation of two macrophases but in terms of 100% conversion of the reactive solvent into polymer.

Considering the morphology development upon curing, an important distinction has to be made between step-growth and chain-growth polymerizations. In all cases curing (polymerization) should start from homogeneous solutions in view of processability and morphology control. In the case of step-growth polymerization, the molar mass of the polymerizing reactive solvent changes continuously with conversion. At 50% monomer conversion, the number-average degree of polymerization is 2, i.e., the main products present are dimers (see Sec. 10.3). Suppose a polymer (P)/reactive solvent (S) system with an upper critical solution temperature (UCST) phase behavior as depicted schematically in Fig. 10-7 B is cured at temperature T_p. The phase behavior will change during the polymerization process due to the increasing molar mass of the polymerizing reactive solvent, i.e., the formation of dimers, trimers, etc. Concomitantly, the L–L demixing curve will shift upwards. Phase separation will occur when the L–L demixing curve shifts to temperatures above T_p. This situation is encountered, for example, in the system PPE/epoxy (see Sec. 10.5).

Let us consider a polymer–reactive solvent system where the reactive solvent is polymerized via a chain-growth polymerization mechanism. Initially, the polymer–reactive solvent system can be considered as a binary system, with a phase diagram as represented by the dashed line in Fig. 10-7 C. Upon polymerization of the reactive solvent, a polymer is formed with a high molar mass, which will not change significantly during polymerization. Concomitantly, a ternary system is formed consisting of polymer–reactive solvent–polymerized reactive solvent (see Fig. 10-7 C). Although the reacting system is not in equilibrium due to the continuous formation of polymer, and moreover because we are dealing with polydisperse polymers, the use of a simple (equilibrium) ternary phase diagram, as shown in Fig. 10-7 C, might be useful for the discussion on the morphology development. The initial composition of the homogeneous solutions is located on the polymer–reactive solvent axis. Upon polymerization, a reaction line is followed as indicated by the dotted-dashed lines (A–A′, B–B′ and C–C′) in Fig. 10-7 C. After a small amount of conversion of the reactive solvent, the binodal line (solid line) is crossed and the system becomes metastable. This might lead to phase separation. However, when the spinodal line (dashed line) is crossed, the system will phase separate. The positions of the binodal and spinodal curves depend on the molar mass of the polymer and polymerized reactive solvents and the interaction parameters between the polymers and the reactive solvent. Considering the case where the interactions between the solvent and both

polymers are identical, the critical point is located at the maximum of the binodal and the corresponding tie lines are horizontal when the polymers have equal molar masses. The examples given above show that for these reactive systems the morphology depends not only on the thermodynamics, but more importantly on the relative rate of phase separation and the rate of polymerization. In the case where the dissolved polymer is amorphous, vitrification can interfere with L–L demixing (see Sec. 10.4.1), while in the case of a semicrystalline polymer, crystallization can interfere with L–L demixing. The occurrence of vitrification/crystallization enables fixation of the nonequilibrium morphologies. When all the reactive solvent has been transformed into polymer, the system can be considered as a binary system again, containing the polymer and the polymerized reactive solvent.

10.5 Example of an Intractable Polymer/Reactive Solvent System: The Poly(phenylene ether) (PPE)/Epoxy System

10.5.1 Materials Choice: PPE/Epoxy

Epoxy resins prove to be surprisingly effective solvents for many polymers, as can be concluded from a literature survey by Venderbosch (Venderbosch, 1995). PPE is chosen for its interesting mechanical properties in terms of a high T_g, a relatively high intrinsic impact strength, and average values for the modulus, yield stress, and breaking strength. Given its high T_g of 220 °C, the processing temperature should be around 350 °C. This, in combination with its limited thermal and oxidative stability, results in severe degradation, and consequently PPE can be considered as a classical example of an intriguing, but intractable polymer.

10.5.2 Phase Behavior of PPE/Epoxy Solutions

In order to estimate the processing window of PPE/epoxy solutions, the phase diagram was investigated first. The phase diagram of PPE–DGEBA was constructed from a combination of light scattering experiments, dynamic mechanical thermal analysis (DMTA), and rheology [for further details see Venderbosch (1995) and Venderbosch et al. (1994, 1995 a, b) and references cited therein]. The resulting phase diagram is presented in Fig. 10-8, from which it can be seen that rather high temperatures are required to reach the region of homogeneous solutions.

The cloud-point curves exhibit a typical upper critical solution temperature (UCST) behavior, commonly observed for poly-

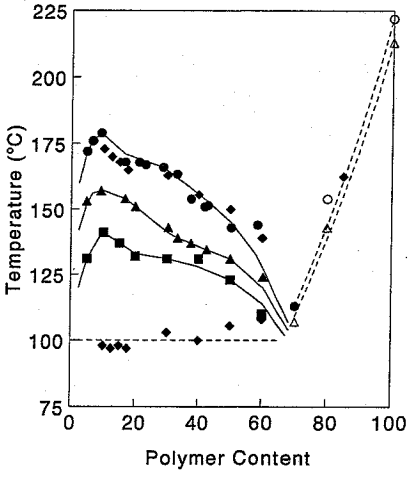

Figure 10-8. Phase diagram of PPE/epoxy solutions as derived from light scattering experiments (closed circles, triangles, and squares), DMTA (open circles), and rheology (closed chevrons). Open and closed circles and closed chevrons: $M_w = 30$ kg/mol; open and closed triangles: $M_w = 18$ kg/mol; closed squares: $M_w = 10$ kg/mol. The solid lines indicate the onset of phase separation, the dashed lines on the right the T_g–composition line of the homogeneous solutions, and the horizontal dashed line with closed chevrons the T_g–composition line of the heterogeneous solutions.

mer–solvent systems. As expected, a decrease in the PPE molar mass enhances the miscibility of the system and results in a considerable shift of the cloud-point surve to lower temperatures. Since PPE as well as the epoxy resin is polydisperse, the cloud-point curves may not be regarded as binodal curves. The inflection in the curves clearly reveals the influence of the molar mass distribution, i.e., the critical point is not situated at the top of the curves. The T_g–composition lines, as determined by DMTA, and as calculated with the Fox equation (using a T_g of 222 and 213 °C for PPE with a molar mass of 30 and 18 kg/mol, respectively, and a T_g of −18 °C for the epoxy monomer), are also given in Fig. 10-8 and they intersect the cloud-point curves at a PPE content of approximately 70%. Thus solutions with less than 70 wt.%

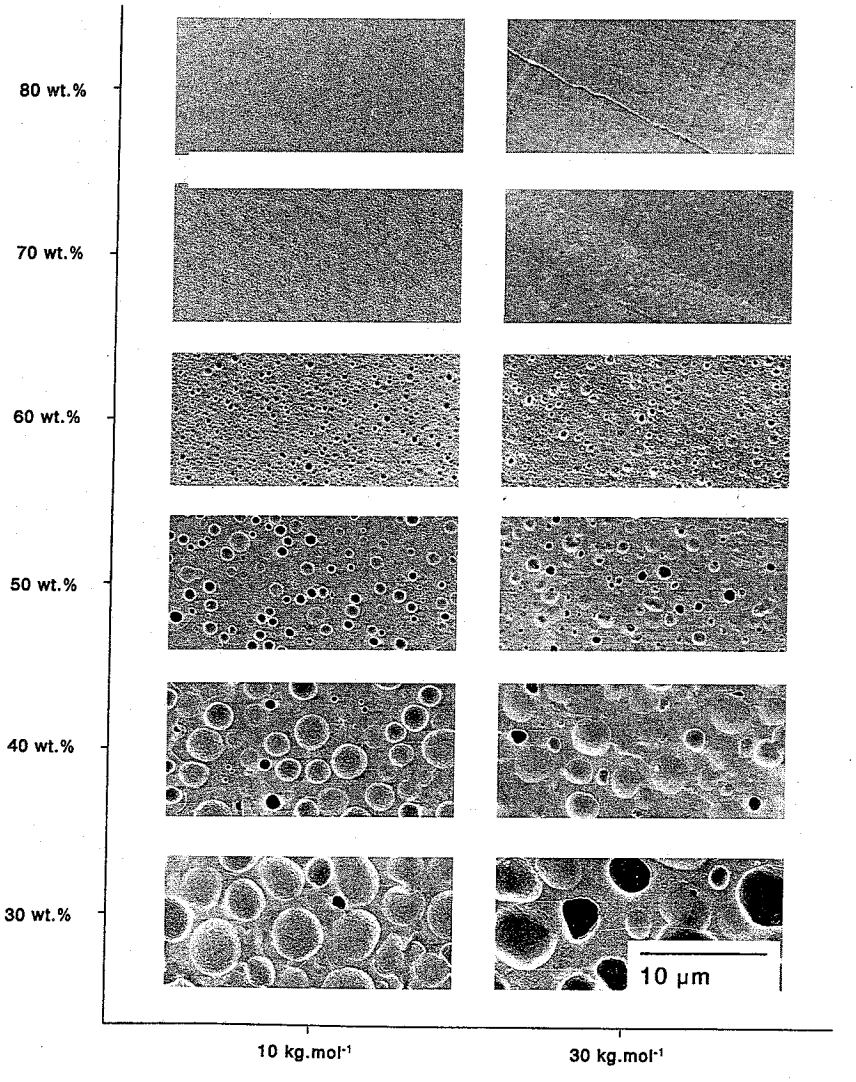

Figure 10-9. Scanning electron micrographs of PPE/epoxy solutions with a PPE molar mass of 10 and 30 kg/mol and a PPE content of 30–80 wt.%, after cooling from 200 °C to room temperature at a rate of 1 °C/min.

PPE will phase separate upon cooling; however, phase separation is not complete but arrested as soon as the PPE-rich phase vitrifies at this intersection point (the Berghmans point, see also Sec. 10.4). As a result of this phenomenon, which can be regarded as a thermo-reversible gelation (TIPS), all of the phase-separated solutions will exhibit a T_g of ~100 °C, as indicated by the dashed horizontal line in Fig. 10-8 and confirmed by rheological experiments. The morphologies resulting from the TIPS (thermally induced phase separation) process are shown in Fig. 10-9. In accordance with the phase diagram in Fig. 10-8, a homogeneously vitrified material is found above 70 wt.% PPE. Below 70 wt.% PPE, dispersed epoxy droplets are observed in a continuous PPE matrix. The size of the dispersed epoxy phase is relatively uniform and depends on the PPE fraction. With increasing PPE content, the viscosity of the solution increases, and consequently during phase separation (TIPS), the coarsening process is retarded with increasing viscosity.

In order to verify the concept of enhanced processability of PPE via the application of epoxy as a reactive solvent, the rheology of PPE/epoxy was investigated. The dynamic rheological behavior of the homogeneous solutions was studied using a Rheometrics RDSII spectrometer [experimental details are mentioned elsewhere, see Venderbosch (1995), and Venderbosch et al. (1994, 1995 a, b) and references cited therein]. The dynamic viscosity as a function of the reduced frequency for the PPE/epoxy solutions with various epoxy contents is shown in Fig. 10-10. The plot shows typical shear thinning behavior, which is commonly observed for semidilute solutions. The expected strong dependence on the volume fraction of the PPE is confirmed. Moderately high zero shear viscosities were found at 200 °C; these are comparable to those of standard thermoplastic polymers. The success of the original aim for intractable PPE is demonstrated by the fact that the processing temperature of PPE was lowered from >300 °C to <200 °C, thus introducing processable PPE.

10.5.3 Curing of PPE/Epoxy Solutions

Curing of PPE/epoxy solutions requires the incorporation of a curing agent which should be compatible with the solution. Aromatic diamines are particularly suitable because of their excellent compatibility with the PPE/epoxy solution. Owing to the addition of a curing agent, which enhances the miscibility of the system, the phase diagram, as shown in Fig. 10-8, is no longer

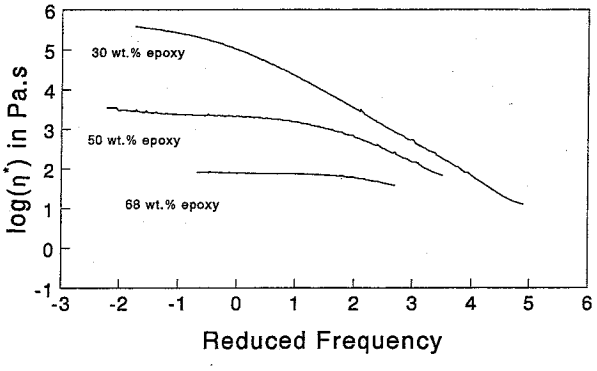

Figure 10-10. Dynamic viscosity versus reduced frequency of PPE/epoxy solutions with epoxy contents of 30, 50, and 68 wt.%, while the molar mass of the PPE used was 30 kg/mol, at 170 °C.

valid. However, it remains useful for indicating the minimal miscibility of the system. Ternary solutions of PPE/epoxy/curing agent still reveal UCST behavior and the absence of phase separation upon cooling at high PPE contents (see Fig. 10-7 B). In ternary solutions, the main driving force for phase separation is the increase in molar mass of solvent into dimer, trimer, etc., induced via step-growth polymerization (curing) (see also Sec. 10.3). As shown by Verchère and co-workers [Verchère et al. (1991) and references cited therein] and de Graaf (1994) for epoxy systems toughened with (in order to prevent phase inversion) relatively small volume fractions of carboxyl-terminated butadiene–acrylonitrile copolymer (CTBN rubber) and polyethersulfone, respectively, minor increases in the molar mass of the solvent significantly reduce the miscibility of the system and phase separation is initiated at relatively low conversions. CIPS can be regarded as inducing a shift and a concurrent change in the shape of the cloud-point curves on the phase diagram towards higher temperatures. The coarseness of the final morphology is controlled, on the one hand, by the competition between the rates of phase separation and coalescence (i.e., diffusion–Ostwald ripening and hydrodynamically driven break-up and coalescence processes), and on the other hand by the rates of vitrification and chemical gelation.

The required compatibility of the curing agents with the PPE/epoxy solutions renders it difficult to estimate their appropriate concentration. For aromatic diamines, the concentration should be equal to the stoichiometric ratio, but an excess is likely to be required in order to compensate for any loss of curing agent due to dissolution in the PPE phase. For this reason the optimal concentration, which is defined as the concentration that results in the highest T_g of the

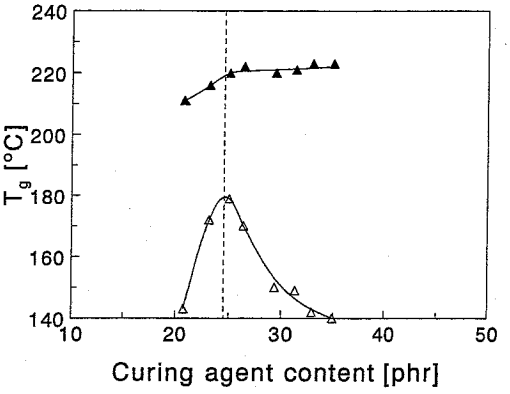

Figure 10-11. Glass transition temperatures versus curing agent concentration of epoxy phase (open triangles) and PPE phase (closed triangles), as determined by DMTA (frequency 1 Hz) for cured blends containing 35 wt.% epoxy, while the molar mass of the PPE was 30 kg/mol.

epoxy phase, was determined using DMTA. Figure 10-11 demonstrates that virtually complete phase separation is obtained, at least for the polymerization temperatures used. This is of essential importance, not only for the expected mechanical properties, but also for the nontoxicity of the final product. The latter is clearly illustrated by the optimal concentration of (generally toxic) curing agent which proves to be very close to, or even equal to, the stoichiometric ratio, as revealed by the pronounced maximum in the epoxy T_g. This can be explained by the fact that a deficiency (incomplete curing) as well as an excess (yielding a more linear polymerization) results in a lower T_g. The morphology of the cured samples is shown in Fig. 10-12 for four volume fractions in the relevant mid-region, prepared by extraction of the PPE matrix. Relatively monodisperse epoxy spheres with a particle size distribution of $D_w/D_n \sim 1.2$ are found (see also Fig. 10-13). This is not a general rule, however, since for some other polymer–reactive solvent systems, such as those recently being investigated in our laborato-

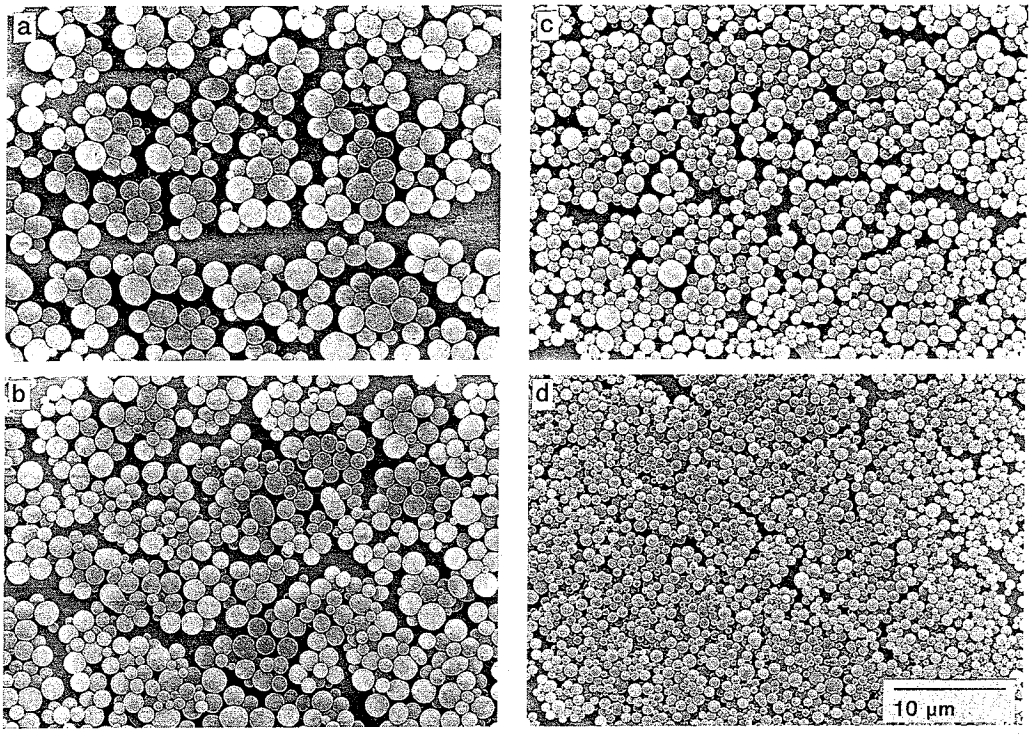

Figure 10-12. Scanning electron micrographs of the dispersed epoxy phase isolated from PPE/epoxy cured at 225 °C with initial compositions of (a) 60, (b) 50, (c) 40, and (d) 20 wt.% epoxy.

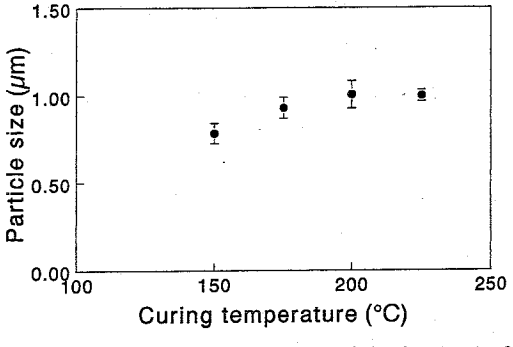

Figure 10-13. Number-average particle size (µm) of PPE/epoxy system as a function of the initial curing temperature for a constant composition of 40 wt.% epoxy.

ry, a distinct dependence on curing temperature and curing rate is sometimes found. This effect becomes increasingly important for semicrystalline polymers, where locking-in of the morphology by crystallization interferes with phase separation (see also Sec. 10.6.2).

10.5.4 Morphology Development

In order to study morphology development, the chemo-rheology of PPE/epoxy/M-CDEA (see Fig. 10-4) was investigated. The dynamic viscosity and loss angle versus time of an isothermally cured PPE/epoxy system are presented with the curing temperature (Fig. 10-14) and the blend composition (Fig. 10-15) as parameters (Venderbosch, 1995; Venderbosch et al., 1994, 1995 a, b).

The onset of phase separation (arrows) and the gradual increase in viscosity due to the formation of a PPE-rich continuous phase are apparent (I). Accordingly, vitrification of this phase (II) and gelation of the

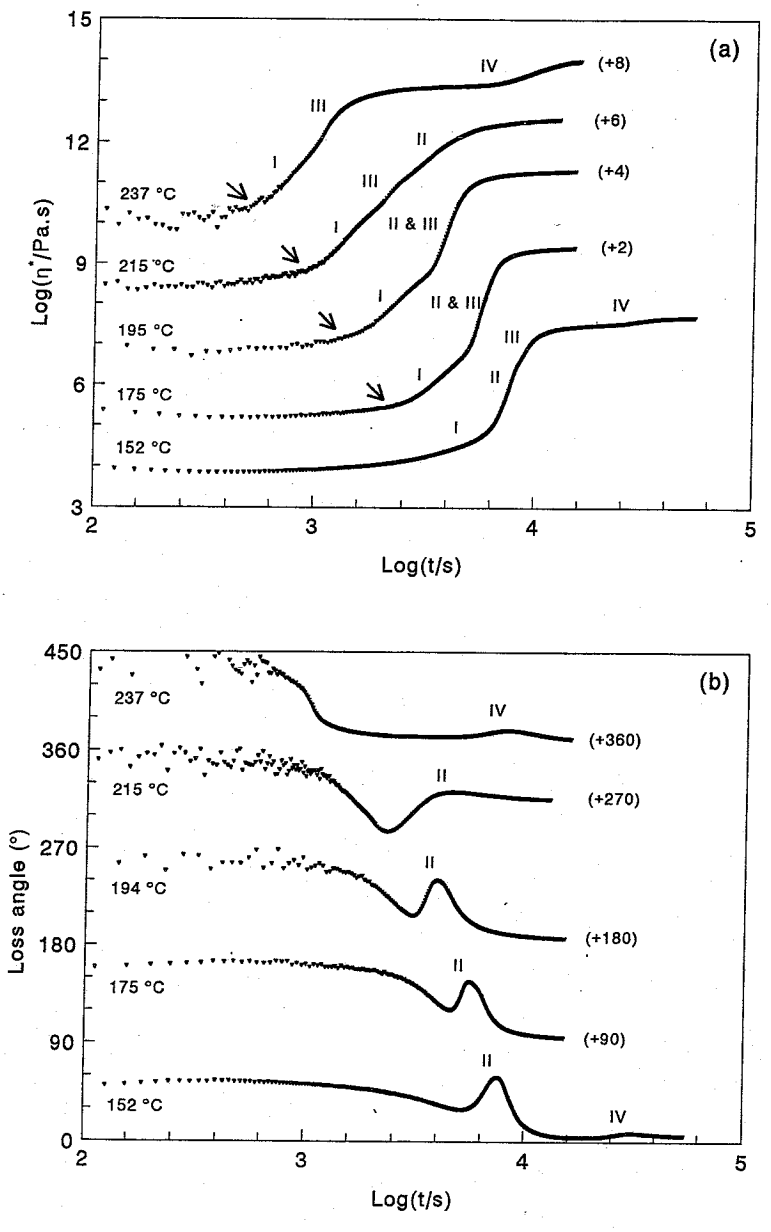

Figure 10-14. Rheology upon isothermal curing of PPE/epoxy (50 wt.% epoxy) versus temperature: (a) dynamic viscosity; (b) loss angle (strain 2%, frequency = 10 rad/s, plate diameter = 8 mm). The arrows indicate the onset of phase separation. (For clarity the curves are shifted upwards by the values indicated in parentheses.)

dispersed epoxy phase (III) are found, although they are usually difficult to distinguish as they happen almost simultaneously, followed by the vitrification of the epoxy phase (IV). At a low temperature, vitrification of PPE occurs before gelation of the epoxy and no interference of the gelation on the final morphology can be expected. At high temperatures this could be the case, although basically only in the case where reaction rates exceed the rate of phase separation, can a pronounced influence be anticipated. In the slow curing system with M-CDEA, this is not the case, and the mor-

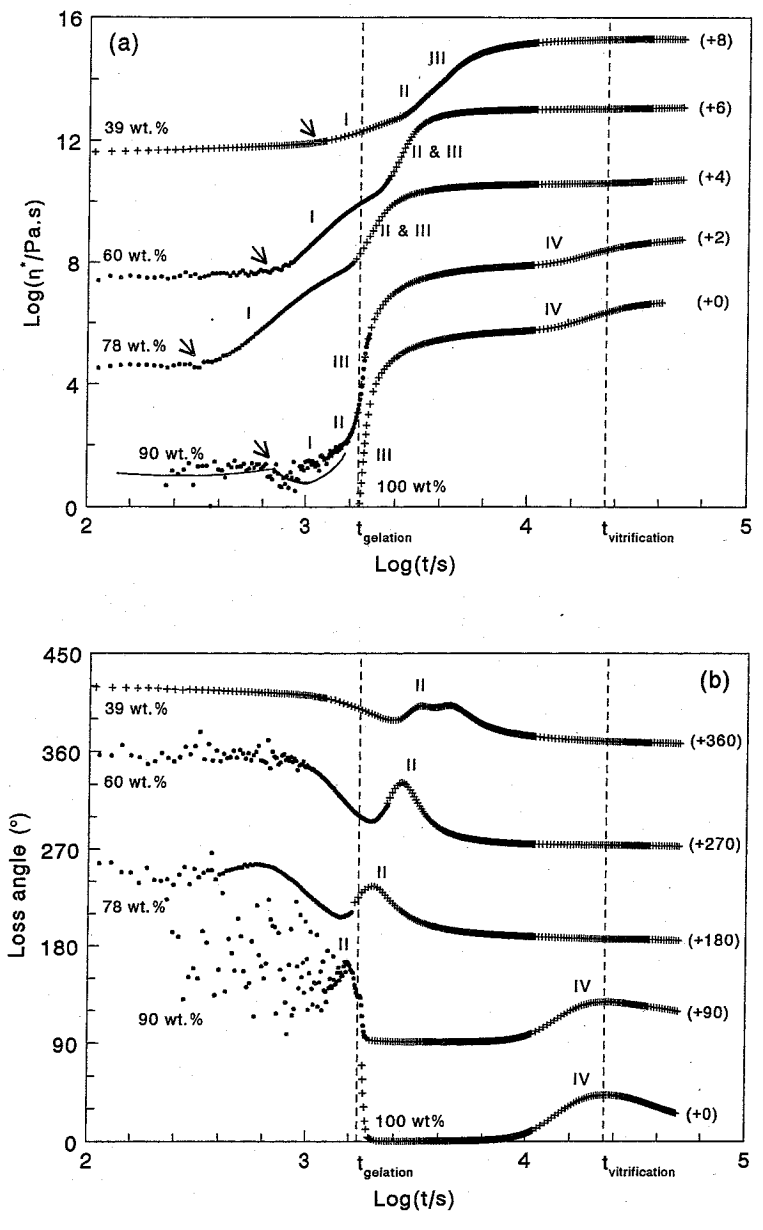

Figure 10-15. Rheology upon isothermal curing of PPE/epoxy at 200 °C versus composition (as indicated in the separate figures): (a) dynamic viscosity; (b) loss angle (strain <2%; 10 rad/s; the plots are a combination of measurements with a plate diameter of 50 mm (-closed circles); 8 mm in the case (+) of the system with 39 wt.% epoxy). The drawn line in Fig. 10-15 a was obtained on a Brookfield rheometer. For clarity the curves are shifted by the values in parentheses. The times, t_{gel} and t_{vitr} of epoxy/M-CDEA are given as reference points.

phology depends uniquely on the viscosity of the matrix at the moment of phase separation.

The composition data in Fig. 10-15 a and b clearly reveal that the minimum time for phase separation occurs with 78 wt.% epoxy, in accordance with UCST behavior, and phase inversion is detected at between 90 and 78 wt.% epoxy, accompanied by a large rise in the viscosity, yielding early matrix vitrification (most pronounced at intermediate polymer concentrations between 78 and 60 wt.% epoxy), and hence the potential for early demolding. In conclu-

sion, rheological measurements prove to provide a useful tool for monitoring the morphology development upon isothermal curing of PPE–epoxy–M-CDEA.

In this system, the morphology is mainly controlled by the formation of a highly viscous, PPE-rich continuous phase during the early stages of the reaction-induced phase separation process. Only at polymerization rates considerably higher than the rate of phase separation is a pronounced influence on the final morphology anticipated.

10.5.5 Mechanical Properties

In order to systematically vary the mechanical properties of the dispersed epoxy phase, the flexibility of the epoxy network was tuned by blending aromatic DGEBA (stiff) and aliphatic DGEPPO (flexible) epoxies (see Fig. 10-4). The glass transition temperatures of the DGEBA/DGEPPO mixtures; 110/0, 80/20, 60/40, 40/60, 20/80, and 0/100, cured with M-CDEA or Jeffamine D-400, are shown in Fig. 10-16. The T_g of the resulting epoxy material gradually decreases from 200 °C to –30 °C, as a unique function of the total polypropylene oxide content. The tensile properties of the final epoxy network reveal the great flexibility obtained by tuning the properties of the epoxy phase from a brittle glass to a ductile or relatively brittle rubber, depending on the position of T_g relative to room temperature [for further details see Venderbosch (1995) and Venderbosch et al. (1994, 1995 a, b) and references cited therein].

The above-mentioned mixtures of DGEBA/DGEPPO were applied as reactive solvents for PPE. The miscibility of

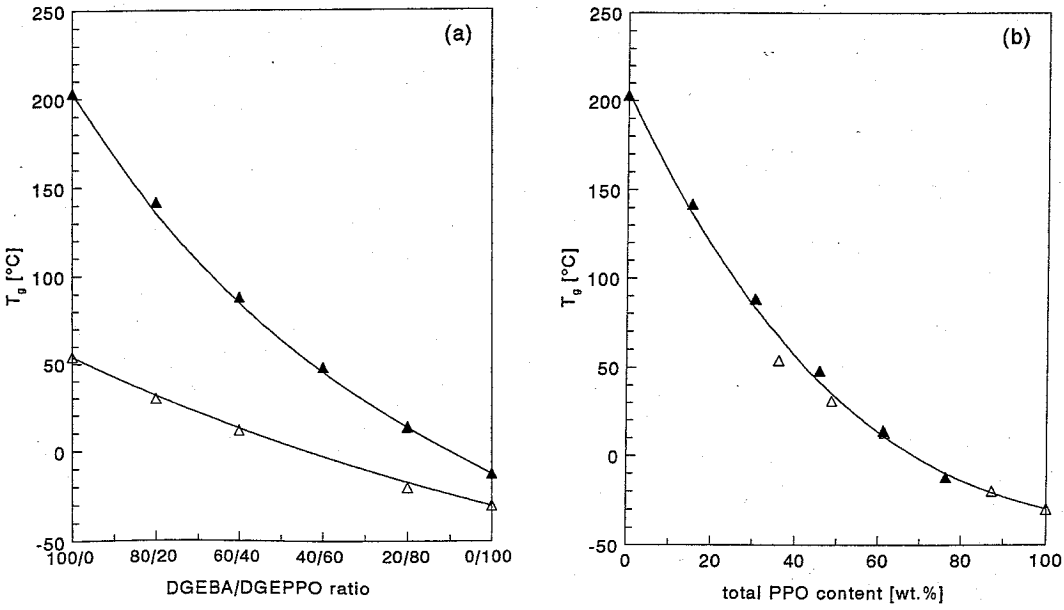

Figure 10-16. Glass transition temperatures, as determined by DMTA, of mixtures of DGEBA and DGEPPO resin cured using M-CDEA (closed triangles) or Jeffamine D-400 (open triangles) versus (a) the DGEBA/DGEPPO ratio and (b) the total polypropylene oxide (PPO) content. Solid lines: Fox equation.

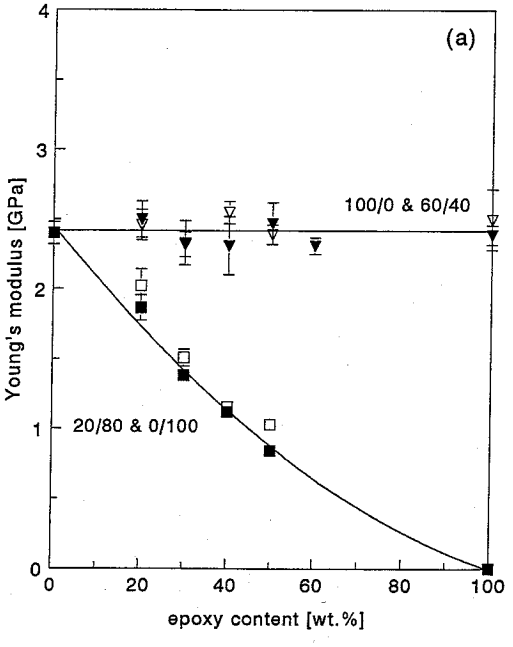

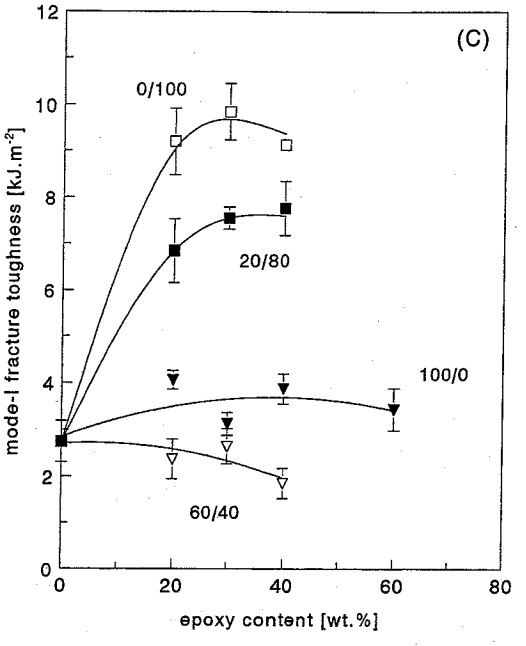

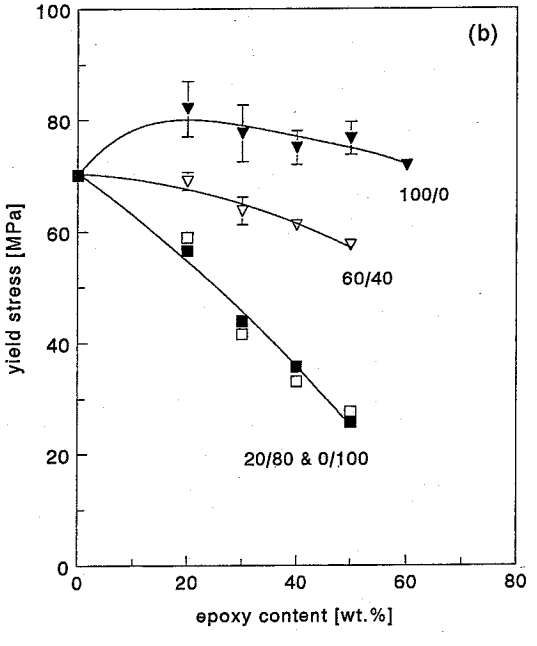

Figure 10-17. Tensile properties of PPE/epoxy versus the epoxy content for DGEBA/DGEPPO ratios of 100/0 (closed triangles), 60/40 (open triangles), 20/80 (closed squares), and 0/100 (open squares): (a) Young's modulus; (b) yield stress; and (c) fracture toughness (G_{Ic}) (testing speed of 1 m/s).

PPE–DGEPPO proved to be decreased relative to PPE–DGEBA, but only a very small shift in the cloud-point curve towards higher temperatures resulted. The morphology of the cured systems proved to be very similar to what we had already found, i.e., micrometer-sized droplets of epoxy in a continuous PPE phase. The main mechanical properties of the total system are summarized in Fig. 10-17, listing the modulus, yield stress, and (high speed) fracture toughness values as a function of the amount of epoxy added, and with the ratio of DGEBA/DGEPPO as a parameter. Indeed the properties can be tuned to requirements but, more interestingly, the reactive solvent, i.e., after being used as a processing aid, is locked up as an integral part of the resulting product, inside the thermoplastic matrix. Its usefulness as a structural element is clearly illustrated by the remarkable toughness enhancement obtained in the already tough PPE when rubbery epoxies are used (see Fig. 10-17 C).

10.5.6 Composite Applications

Making use of these newly developed polymer systems, high T_g thermoplastic composites were prepared using the film stacking technology. By introducing epoxy resin(s) as a reactive solvent, the flow became sufficiently high to fully wet and impregnate the fibers, yielding composite materials of high quality (Venderbosch, 1995; Venderbosch et al., 1994, 1995 a, b). Microscopic analysis revealed an interesting composite morphology, i.e., the epoxy phase tends to accumulate at polar surfaces such as those of glass and surface-treated carbon fibers (see Fig. 10-18). Remarkably, this phase segregation is almost complete in the case of high fiber loadings, and, for a fiber volume fraction of 50%, a morphology of epoxy-coated fibers in a pure PPE matrix is found (see Fig. 10-18). This (unique) morphology is not only of great importance with respect to the possibility of drastically improving the strength of the interphase or the level of adhesion between fibers and matrix, but also offers the potential to individually coat fibers with a thick and adjustable (e.g., glassy or completely rubbery) interphase. Apart from the apparent influence of the fiber volume fraction or the fiber spacing, a prerequisite for complete phase separation to occur is that sufficient mobility and time exist for completion of this diffusion process. For the fixed reaction rate of the system, the viscosity of the matrix plays a dominant role. If more than 30% epoxy is present, complete phase separation to the fiber surface is achieved and a nearly neat PPE matrix results (see Fig. 10-19). This is confirmed by transverse flexural strength tests on unidirectional composites which show that the maximum properties are obtained as soon as a continuous epoxy interphase is formed (see Fig. 10-20).

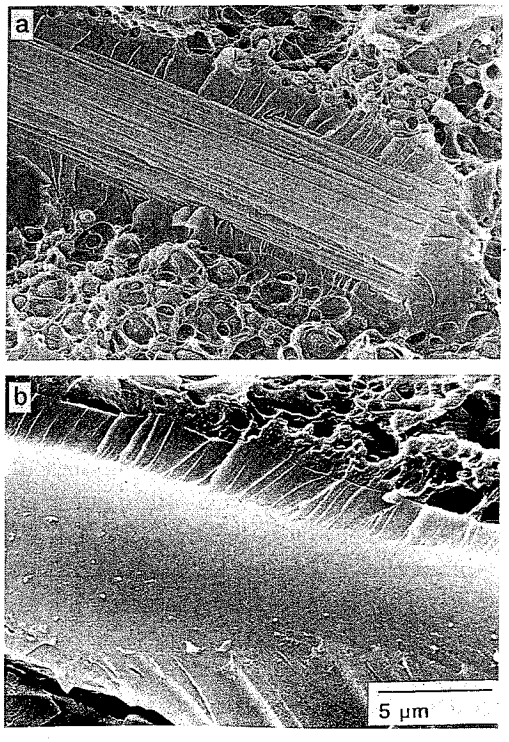

Figure 10-18. SEM micrographs of fracture surfaces of short-fiber-reinforced composites (17 vol.% fibers) based on PPE/epoxy (56 wt.%, 25 phr Ethacure 100): (a) Grafil X-AS carbon fiber; (b) E-glass fiber.

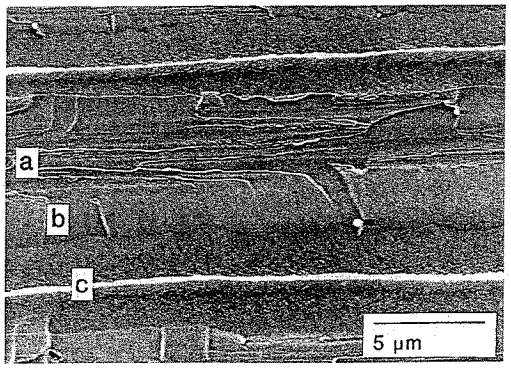

Figure 10-19. SEM micrographs of the fracture surface in a fiber-rich area of PPE/epoxy-based (40 wt.% epoxy, 55 phr M-CDEA) carbon-fabric reinforced composite (50 vol.% fiber): (a) fiber (imprint); (b) epoxy layer; (c) PPE matrix.

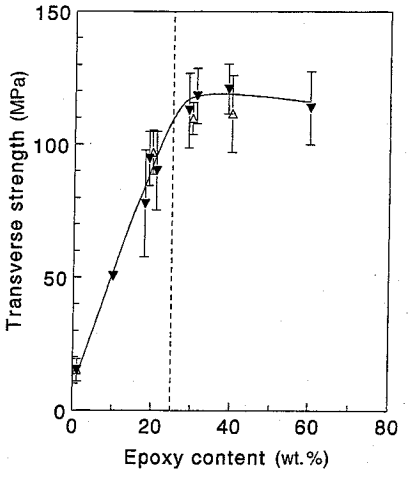

Figure 10-20. Transverse flexural strength (MPa) of unidirectional PPE/epoxy composites with a fiber volume fraction of 50 (open triangles) and 60% (closed triangles) versus the epoxy (DGEBA) content (wt.%) of the matrix.

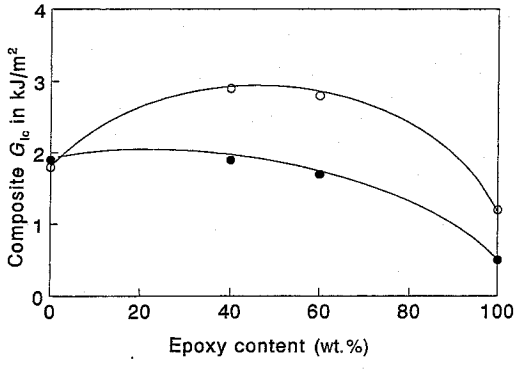

Figure 10-21. Critical strain energy release rate G_{Ic} of carbon-fabric reinforced composites (50 vol.% fibers) versus the matrix composition: mode I (closed circles) and mode II (open circles).

Of all the properties measured [with typical values for the flexural moduli of 40 GPa and strength values of 0.7 GPa for this high T_g (220 °C), thermoplastic, 50% carbon-fabric-reinforced composite], the impact properties proved to be the most interesting, as shown by the mode I and II critical strain energy release rates given in Fig. 10-21, and the C-scan results after impact (see Fig. 10-22). The synergy found in the mode II results can be explained by an apparent optimal combination of brittle and ductile matrix components. The brittle epoxy phase, enclosing all the fibers, not only yields a strong and well adhering interphase, but also induces an increase of the deformation area of the crack and, consequently, of the level of toughness, assuming that cracks in the epoxy coating can initiate yielding in the adjacent PPE matrix. Since the mode II results of the interlaminar fracture toughness tests relate linearly to the values of the practical (Boeing) compressive strength after impact (CSAI) (Cantwell and Morton, 1991), they are of great practical importance. Possibly, by the introduction of these brittle interphases, a method has been found to toughen fiber-reinforced composites, with a ductile thermoplastic matrix, beyond the usual limits imposed by the presence of rigid fibers.

The continuous variation of the properties of the interphases from glassy to rubbery can be realized by mixing DGEBA with DGEPPO. Consequently, the macroscopic properties of the composites are strongly influenced. Glassy interphases were shown to be in favor of structural applications (mode II fracture toughness). On the other hand, by increasing the ductility of the interphases, mode I fracture toughness is favored; superior Charpy impact values were obtained and the transverse strength and strain-at-break were significantly improved. However, these ultimate transverse properties were obtained at the expense of the compressive properties, due to the low shear modulus of the interphase. By changing the viscosity and the chemistry of the systems employed, e.g., by using end-modified, low molar mass PPEs which can co-react with the reactive solvent, the existing limits with respect to the diffusion-

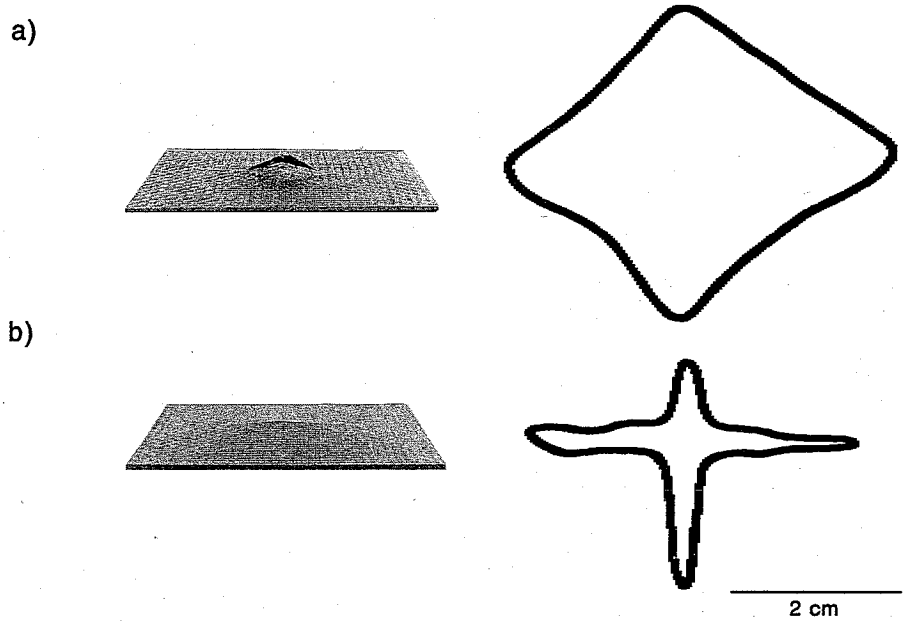

Figure 10-22. Tensile face damage and schematic representation of C-scan images of carbon-fabric laminates (50 vol.% fibers) impacted at an energy level of 9 J: (a) epoxy matrix; (b) PPE/epoxy matrix (40 wt.% epoxy).

controlled, complete phase separation could be surpassed, and thinner interphases could be realized.

10.6 Examples of Tractable Polymer/Reactive Solvent Systems

In this section, two polymer–reactive solvent systems will be discussed, in which the polymer is either amorphous (PMMA) or semicrystalline (HDPE), while the reactive solvent is polymerized via a step-growth (epoxy resin) or a chain-growth (styrene) polymerization, respectively.

10.6.1 The Poly(methylmethacrylate)/ Epoxy System

Poly(methylmethacrylate) (PMMA) is an amorphous glassy polymer possessing a T_g of approximately 110 °C. Like polystyrene, PMMA is brittle, with a low strain-at-break and a poor impact performance. Upon deformation of PMMA and PS, crazing occurs on a microscale and the small cracks which appear in the material, perpendicular to the stress direction, are bridged by numerous fibrils. The maximum elongation of these craze fibrils approaches the theoretical limit estimated from the maximum draw ratio of an entanglement network, as shown by Kramer and Donald (1982). For example, the molar mass between entanglements in the case of polystyrene is approximately 20 kg/mol and, assuming that no chain slippage occurs through entanglements, the maximum draw ratio should be of the order of 4, or equivalently a strain-at-break of 300%. In practice, however, polystyrene is the paradigm of a brittle material with a macroscopic strain-at-break of 1–3%. This paradox, a polymer possessing a loose entanglement network and a low macroscopic strain-at-break, is discussed exten-

sively by van der Sanden in Chap. 12 of this Volume. For the present discussion, we simply summarize that polystyrene is ductile below a certain critical thickness, or equivalently below a certain interparticle distance (D_{Ic}). In Chap. 12, Sec. 12.9, it is mentioned that submicrometer engineering foams, i.e., materials possessing holes, or equivalently nonadhering submicrometer (rubbery) particles, with an interparticle distance below D_{Ic}, are a great challenge for the future for toughening brittle glassy polymers. In this respect, PMMA was mentioned as an interesting candidate in addition to polystyrene (see Chap. 12, Sec. 12.9).

In a recent Dutch patent application (Jansen and van der Sanden, 1996), the processing route involving reactive solvents was used to make tough and transparent PMMA via two routes. In route 1 PMMA was dissolved in an epoxy resin, and in route 2 the monomer MMA was dissolved in epoxy resin. In order to obtain finely dispersed rubbery particles in a PMMA matrix via route 1, the polymerization temperature proved to be crucial. It was stated that the polymerization temperature T_p should be limited by

$$T_g\,(\text{PMMA/epoxy}) - 20\,^{\circ}\text{C} < T_p < T_g\,(\text{PMMA/epoxy}) + 20\,^{\circ}\text{C} \quad (10\text{-}3)$$

As shown by Eq. (10-3), the T_gs of solutions depend on the composition, i.e., in the case of epoxy/PMMA solutions, the T_g will increase during polymerization as a consequence of the conversion from epoxy resin (the solvent for PMMA) into a thermoset

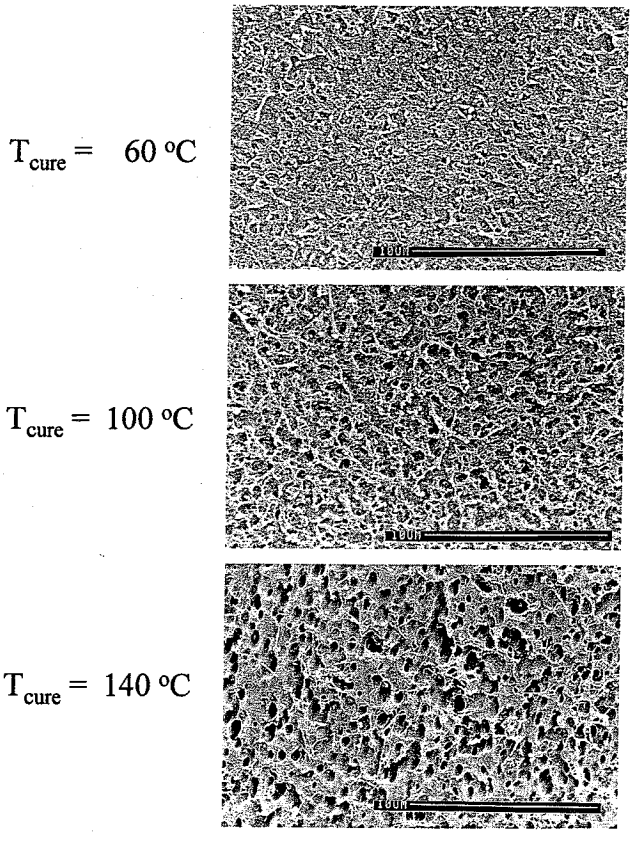

Figure 10-23. The effect of curing temperature on the morphology of the final blend of 70 wt.% PMMA and 30 wt.% epoxy.

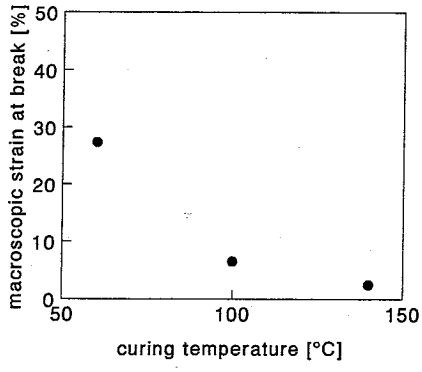

Figure 10-24. Macroscopic strain-at-break of PMMA–epoxy (70/30) blend for different curing temperatures.

epoxy which is immiscible with PMMA. The morphology is the result of the rate of polymerization versus the rate of coalescence of the dispersed polymerizing epoxy phase. The more viscous the solution, i.e., the closer to its T_g, the less coalescence is to be expected. In actual practice, it is rather difficult to follow the T_g of the system from the reaction temperature profile, and, as a compromise, the curing of epoxy in the case of PMMA/epoxy systems is performed at a low temperature, i.e., at a relatively high viscosity. The effect of the curing temperature is striking. This is demonstrated in Fig. 10-23, where the lower the polymerization temperature, the finer the particle sizes of the dispersed epoxy particles. In Fig. 10-24, the corresponding mechanical properties are shown and it can be seen that the strain-at-break increases with decreasing particle size, or equivalently a smaller interparticle distance.

10.6.2 The Polyethylene/Styrene System

In contrast with the polyphenylene ether/epoxy system, where a reactive solvent is used to lower the processing temperature, the use of a reactive solvent in the case of high-density polyethylene (PE) is aimed at lowering the viscosity. In this case, the low viscosity solution can be cast or even poured into a mold, which might be advantageous for making large and complex structures, e.g., connectors for the cable industry. The system polyethylene/styrene is discussed below, but we hasten to add that the PE/styrene system is only used to serve the purpose of demonstrating the structural changes that take place as a result of CIPS (L–L) combined with crystallization (L–S). In actual practice, styrene is not a desirable solvent in view of environmental legislation, but other solvent systems are possible, e.g., methacrylates. A detailed study concerning the system PE/styrene has been carried out Goossens and co-workers and is published extensively in his Ph.D. thesis (Goossens et al., 1996). Some salient features are described below.

10.6.2.1 Miscibility of Polyethylene and Styrene

As discussed in Sec. 10.4, it is of importance to know the phase behavior of the polymer/solvent system to be processed. The experimental melting (dissolution) and crystallization curves of polyethylene (in this case a linear polyethylene possessing a molar mass, M_w, of 75 kg mol^{-1}) in styrene, as a function of the composition, are shown in Fig. 10-25. Experimental melting or dissolution curves are commonly analyzed using the well-known melting point depression relationship based on the Flory–Huggins lattice theory [see Eq. (10-2)].

As can be discerned from Fig. 10-25, there is no indication of interference with L–L demixing, as reported by Richards (1946), Roginova and Slonimskii (1974), and Nakajima et al. (1966) for several PE–solvent systems. In conclusion, styrene is a good solvent for PE at elevated temperatures (Goossens et al., 1996).

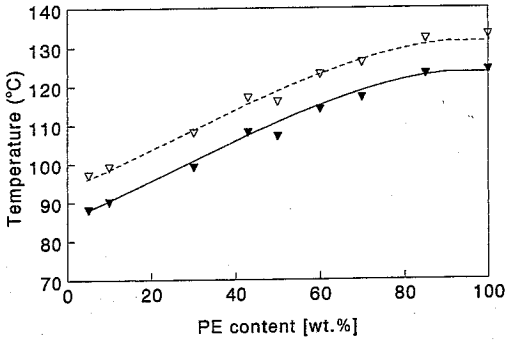

Figure 10-25. Experimental (▽) and calculated (▼) equilibrium melting temperatures as a function of the composition using literature values for the various parameters in Eq. (10-2).

10.6.2.2 Morphology Development as Revealed by Small Angle X-Ray Scattering (SAXS) and Wide Angle X-Ray Scattering (WAXS)

In situ simultaneous SAXS and WAXS data collected during isothermal polymerization at the Synchroton Radiation Source (SRS) in Daresbury (U.K.), during isothermal polymerization, are shown in Fig. 10-26 at two temperatures, 120 and 125 °C, respectively. At a polymerization temperature, T_p, of 125 °C, no crystallization is expected (see also Fig. 10-25), since T_p is above the crystallization curve and only L–L demixing can occur during polymerization. At a polymerization temperature of 120 °C, crystallization can occur at a later stage of the polymerization process when the crystallization temperature of PE in residual styrene exceeds T_p (see also Fig. 10-25).

The SAXS data (see Fig. 10-26 A, C, E, and F) are presented as three-dimensional plots of intensity, $I(q)$, versus the scattering, vector, $q = (4\pi/\lambda) \sin \theta$, where 2θ is the scattering angle, as a function of the polymerization time. The WAXS data for the polymerization temperature of 120 °C are presented in Fig. 10-26 B and D as three-dimensional plots of intensity, $I(2\theta)$, versus the scattering angle 2θ, versus time. All the SAXS patterns in Fig. 10-27 A, C, E, and F initially show little scattering, indicative of homogeneous solutions, as is to be expected from the phase diagram (Fig. 10-25). During polymerization, all of the scattering patterns gradually change. At a polymerization temperature of 120 °C, the WAXS pattern observed at a later stage of the polymerization process shows the characteristics 110 and 200 reflections and the reflections of the higher orders of the orthorhombic PE unit cell (see Fig. 10-26 B and D). No WAXS pattern is observed at 125 °C, as explained above. There is a noticeable difference between the development of the scattering patterns of the 20 and 60 wt.% PE/styrene solutions at 120 °C. For the 20 wt.% systems, a monotonically decaying pattern is observed, and careful analysis showed (Goossens et al., 1996) that the intensity is linearly dependent on the square of time, indicative of a nucleation and growth mechanism (binodal decomposition), according to Lipatov et al. (1985). The 60 wt.% solution, on the other hand, shows a distinct maximum moving to lower q values with increasing polymerization time. This periodic microstructure could be indicative of a spinodal-type of phase-separation process. According to the (linearized) Cahn–Hilliard theory (Cahn, 1963), concentration fluctuations with a dominant wave number will grow giving rise to a periodic microstructure. More detailed information was obtained by Goossens by analyzing the data based on a simple two-phase model and making use of the experimental invariant Q, defined as $Q = \phi_1 \phi_2 / (\rho_1 - \rho_2)^2$, where ϕ is the volume fraction and ρ is the electron density. For the 20 wt.% PE systems, a maximum in the experimental invariant is found in the early stages of the

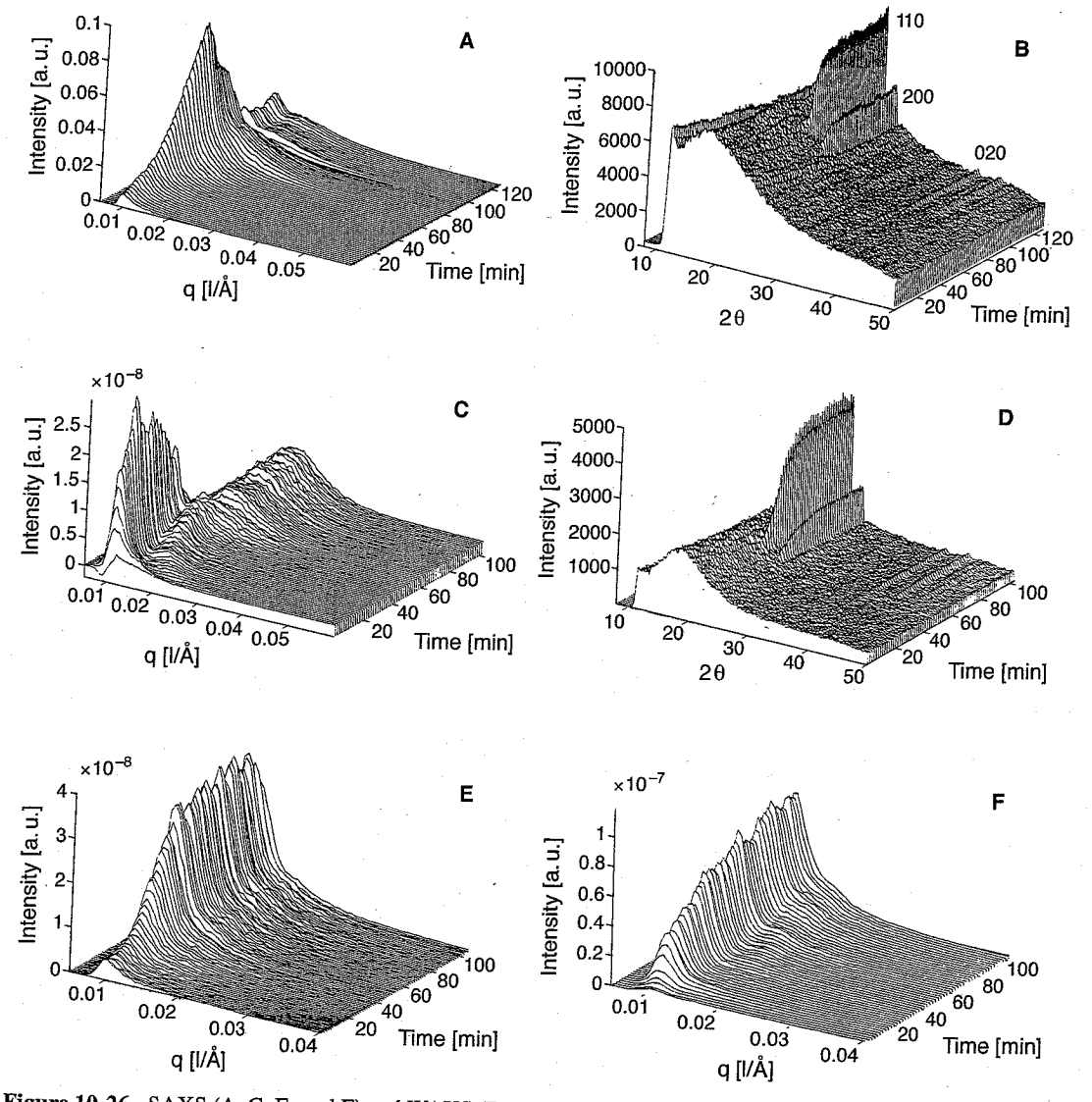

Figure 10-26. SAXS (A, C, E, and F) and WAXS (B and D) data collected during isothermal polymerization at 120 °C (A, B, C, and D) and 125 °C (E and F) for different polyethylene contents (20 wt.% PE in A, B, and E, and 60 wt.% in C, D, and F).

L–L phase separation. Because the electron density contrast, $(\rho_1 - \rho_2)$, between the PE-rich and PS-rich regions only increases during the polymerization, the maximum must be attributed to changes in the volume fractions of the two phases. The volume fraction of the PE-rich phase ranges from 1.0 before the onset of L–L phase separation to final value of 0.2. The invariant reaches a maximum close to equal phase volumes. For the polymerization at 120 °C, a second maximum in the invariant is observed. This originates from the crystallization of PE. The experimental invariants of the 60 wt.% PE systems do not show a maximum, because the phase volumes do not become equal.

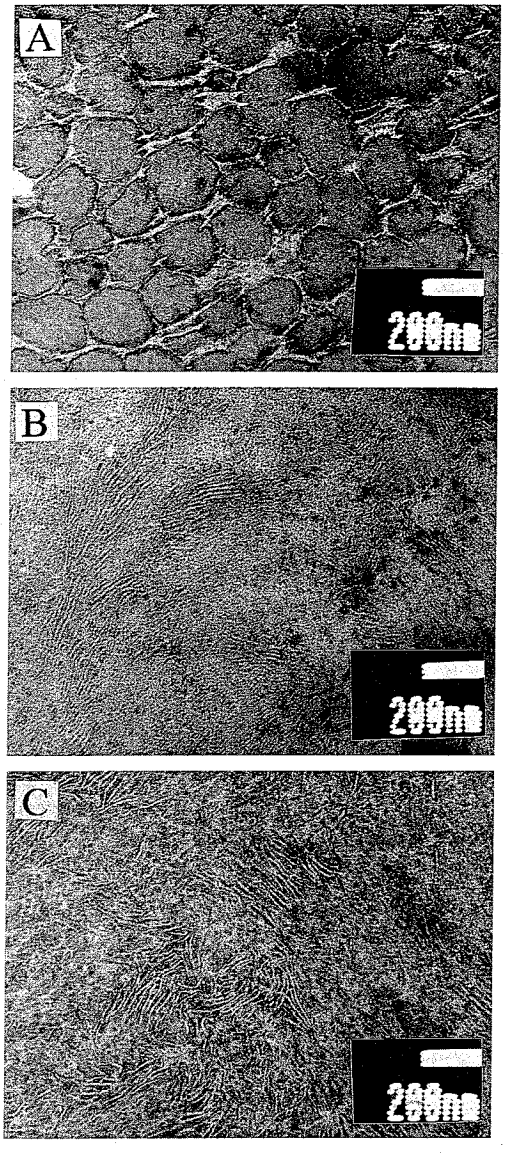

Figure 10-27. Transmission electron micrographs showing the polyethylene/polystyrene blends after complete polymerization at 120 and 125 °C, respectively: (A) polystyrene particles dispersed in a polyethylene matrix obtained by polymerization at 120 °C with 20 wt.% PE in styrene; (B) as (A), but at a higher PE concentration of 60 wt.% and (C) 60 wt.% at 125 °C.

10.6.2.3 Morphology as Revealed by Electron Microscopy

Some representative TEM micrographs of PE/PS blends are presented in Fig. 10-27 A, B, and C. The micrograph of the 20 wt.% PE system (Fig. 10-27 A) clearly shows a phase-separated and phase-inverted morphology of dispersed PS particles in a matrix of PE. Considering the polydispersity of the PS particles size, the morphology is the result of a binodal type of phase separation, as discussed in the previous section. The micrographs of the 60 wt.% PE systems clearly show the difference between the phase-separation mechanisms (see Fig. 10–27 B and C). For this system, the PS is not dispersed as isolated particles, but the co-continuous-like structures confirm the X-ray observations of spinodal-like phase separation.

10.7 Concluding Remarks and Future Outlook

The processing of polymers using reactive solvents (monomers) is an extremely versatile technique with respect to the creation of unique morphologies. In the case of amorphous polymers, as illustrated previously for the PPE/epoxy system, the dispersed epoxy phase can migrate to the fiber surface upon curing the PPE/epoxy resin in the presence of (polar) fibers. In the case of PMMA/epoxy, the particle size of the dispersed thermoset epoxy phase can be controlled by optimizing the polymerization temperature, resulting in tough and transparent PMMA/epoxy blends. In the case of a crystalline polymer, as shown for the polyethylene/styrene system, a multitude of structures can be created by the proper choice of the phase-separation processes, i.e., liquid–liquid or liquid–solid demixing.

In this chapter, although only a few examples were presented, it is clear that in the near future many more systems will be explored in view of the many possibilities for dissolving both intractable and tractable polymers in reactive solvents. In addition, the process is not limited to polymers/reactive solvents but monomers can be considered as well, for example, MMA/epoxy (resins) or caprolactam/PPE (where nylon-6 forms the continuous phase). Moreover, the ultimate need for complete conversion, as is essential in standard reactive processing techniques, is altered in the present processing techniques. After molding, the system can usually be vitrified and postcured outside the mold, permitting the feasibility of short(er) cycle times.

At present, the processing of polymers with reactive solvents is limited to *in mold* casting and curing (polymerization). The process is based on CIPS and phase inversion, which take place in the mold during polymerization. This in-mold operation differentiates our processing route from seemingly identical processes, at least from a physical chemistry point of view, involving chemically induced phase separation and phase inversion, which occur in the reactor. For example, a classical approach to toughen glassy polymers like polystyrene is to dissolve polybutadiene rubber in styrene monomer (high-impact polystyrene) (Rodriguez, 1983). During polymerization, grafting and phase separation occur. Due to grafting, the morphology is fixed, which is essential in view of the fact that the morphology within the pellets should survive the subsequent processing step by the converter (see also Sec. 10.2.3).

10.8 References

Arnauts, J., Berghmans, H. (1987), *Polymer 28,* 66.

Arnauts, J., Berghmans, H., Koningsveld, R. (1993), *Makromol. Chem. 194,* 77.

Berghmans, H., Arnauts, J. (1987), *Polymer 28,* 97.

Bikales, N. M. (1985), in: *Encyclopedia of Polymer Science and Engineering,* 2nd ed., Vol. 3: Mark, H. F., Bikales, N. M., Overberger, C. G., Menges, G. (Eds.). New York: Wiley, p. 549.

Blackwell, J., Biswas, A. (1987), in: *Developments in Oriented Polymers-2:* Ward, I. W. (Ed.). Amsterdam: Elsevier Applied Science, pp. 153–199.

Cahn, J. W. (1963), *J. Chem. Phys. 42,* 93.

Cantwell, W. J., Morton, J. (1991), *Composites 22,* 347.

Ciferri, A. (1987), in: *Developments in Oriented Polymers-2:* Ward, I. M. (Ed.). Amsterdam: Elsevier Applied Science, p. 79.

Couchman, P. R. (1983), *Macromolecules 16,* 1924.

de Graaf, L. (1994), Ph. D. Thesis, University of Twente, The Netherlands.

Flory, P. J. (1956), *Principles of Polymer Chemistry.* Ithaca, NY: Cornell University Press.

Fox, T. G. (1956), *Bull. Am. Phys. Soc. 2,* 123.

Fujita, H. (1990), in: *Studies in Polymer Science,* Vol. 9. Amsterdam: Elsevier.

Garg, A. C., Mai, Y. (1988), *Compos. Sci. Technol. 31,* 179.

Goossens, H., Rastogi, S., Meijer, H. E. H., Lemstra, P. J. (1996), unpublished.

Hedrick, J. C., Patel, N. M., McGrath, J. E. (1993), *Adv. Chem. Ser. 223,* 293.

Jansen, B. J. P., van der Sanden, M. C. M. (1996), Dutch Patent Application.

Koningsveld, R., Stockmayer, W., Nies, E. L. F. (1996), *Thermodynamics of Polymer Systems,* Vol. I, *Phase Diagrams.* Oxford: Oxford University Press, in press.

Kramer, E. J., Donald, A. M. (1982), *Polymer 23,* 461; *23,* 1183.

Levita, G. (1989), *Adv. Chem. Ser. 222,* 93.

Lipatov, Y. S., Grigor'yeva, O. P., Kovernick, G. P., Shilov, V. V., Sergryeva, L. M. (1985), *Makromol. Chem. 186,* 1401.

Mülhaupt, R. (1990), *Chimia 44,* 43.

Nakajima, A., Fujiwara, H., Hamada, F. J. (1966), *Polym. Sci.: Part A2, 4,*507.

Nelissen, L., Meijer, E. W., Lemstra, P. J. (1992), *Polymer 33,* 3734.

Nies, E., Berghmans, H. (1996), private communications.

Pearson, R. A. (1993), *Adv. Chem. Ser. 223,* 405.

Richards, R. B. (1946), *Trans. Faraday Soc. 42,* 10.

Rodriguez, F. (1983), *Principles of Polymer Systems.* New York: McGraw-Hill.

Roginova, L. Z., Slonimskii, G. L. (1974), *Russian Chem. Rev. 43,* 1102.

Smith, P. (1976), Ph. D. Thesis, Groningen.

Sperling, L. H. (1994), *Adv. Chem. Ser. 239,*3.

Stoks, W., Berghmans, H. (1991), *J. Polym. Sci.: Part B: Polym. Phys. 29,* 609.
Stoks, W., Berghmans, H., Moldenaers, P., Mewis, J. (1988), *Br. Polym. J. 20,* 361.
Thayer, A. M. (1995), *Chem. Eng. News 11,* 15.
Vandeweerdt, P., Berghmans, H., Tervoort, Y. (1991), *Macromolecules 24,* 3547.
Venderbosch, R. W. (1995), Ph. D. Thesis, Eindhoven.
Venderbosch, R. W., Meijer, H. E. H., Lemstra, P. J. (1994), *Polymer 35,* 4349.
Venderbosch, R. W., Meijer, H. E. H., Lemstra, P. J. (1995 a), *Polymer 36,* 1167.
Venderbosch, R. W., Meijer, H. E. H., Lemstra, P. J. (1995 b), *Polymer 36,* 2903.
Verchère, D., Pascault, J. P., Sautereau, H., Moschiar, S. M., Riccardi, C. C., Williams, R. J. J. (1991), *J. Appl. Polym. Sci. 43,* 293.